

Fermionic Mean-Field Theory as a Tool for Studying Spin Hamiltonians

Thomas M. Henderson,^{1,2,*} Brent Harrison,³ Ilias Magoulas,⁴ Jason Necaie,³ Andrew M. Projansky,³ Francesco A. Evangelista,⁴ James D. Whitfield,^{3,5} and Gustavo E. Scuseria^{1,2}

¹*Department of Chemistry, Rice University, Houston, Texas 77005, USA*

²*Department of Physics and Astronomy, Rice University, Houston, Texas 77005, USA*

³*Department of Physics and Astronomy, Dartmouth College, Hanover, New Hampshire 03755, USA*

⁴*Department of Chemistry and Cherry Emerson Center for Scientific Computation, Emory University, Atlanta, Georgia 30322, USA*

⁵*AWS Center for Quantum Computing, Pasadena, California 91125, USA*

(Dated: December 10, 2024)

The Jordan–Wigner transformation permits one to convert spin 1/2 operators into spinless fermion ones, or vice versa. In some cases, it transforms an interacting spin Hamiltonian into a noninteracting fermionic one which is exactly solved at the mean-field level. Even when the resulting fermionic Hamiltonian is interacting, its mean-field solution can provide surprisingly accurate energies and correlation functions. Jordan–Wigner is, however, only one possible means of interconverting spin and fermionic degrees of freedom. Here, we apply several such techniques to the XXZ and J_1 – J_2 Heisenberg models, as well as to the pairing or reduced BCS Hamiltonian, with the aim of discovering which of these mappings is most useful in applying fermionic mean-field theory to the study of spin Hamiltonians.

I. INTRODUCTION

It is textbook material [1, 2] that the Jordan–Wigner (JW) transformation [3] can convert certain interacting Hamiltonians of spin 1/2 systems into noninteracting (therefore exactly solvable) Hamiltonians of spinless fermions. Perhaps less appreciated is that even when the JW transformation produces an interacting fermionic Hamiltonian, it can nevertheless be solved at the mean-field level with moderate computational cost and good accuracy [4–13].

Historically, the JW mapping was the first transformation used to relate spin 1/2 objects to fermions. Recently, the prospect of simulating fermionic systems on quantum devices has reignited interest in such mappings [14–17], largely due to the parallels between qubits and spin 1/2 systems. Representing many-fermion problems on a quantum computer requires a mapping from fermions to qubits. Although the inverse JW transformation is a natural choice for this purpose, the past several years have seen the development of a variety of alternatives [14, 18–28].

In this work, we focus on a subset of these alternative mappings and apply them in the other direction. That is, given a transformation converting spinless fermions to spin 1/2 objects, we can invert the mapping to convert spin 1/2 objects to spinless fermions, thereby enabling the solution of interacting spin Hamiltonians using fermionic methods. Of course, the inversion of these mappings is not an entirely trivial task and the resulting fermionic Hamiltonians can be very exotic, but we aim to survey the landscape and discern which, if any, of the many spin-to-fermion mappings we will consider might be particularly useful.

To help orient the reader, we will begin with a quick survey of the spin-to-fermion transformations that we will consider in this work. We certainly cannot do full justice to this topic here, but we hope to provide a reasonably concise summary of these ideas. Likewise, because the Hamiltonians we obtain after the spin-to-fermion transformation are generally quite unusual, we must employ equally unusual mean-field methods to solve them, and we also provide a brief introduction to the general Hartree–Fock–Bogoliubov–Fukutome (HFBF) mean-field theory [29–32] we use to tackle these problems.

II. SPIN-TO-FERMION TRANSFORMATIONS

The Hilbert space for a spin 1/2 object is spanned by two states: $|\uparrow\rangle$ and $|\downarrow\rangle$. The same is true for the Hilbert space of a spinless fermion, spanned by states $|0\rangle$ and $|1\rangle$ in the occupation number representation. Since the Hilbert spaces have the same size, we can map states for a single spinless fermion onto states for a single spin 1/2, and vice versa. The only real difficulty in extending these ideas to map states for M fermions onto states for M spins is that operators acting on different fermions anticommute, while operators acting on different spins commute. This idea was discussed by Jordan and Wigner in 1928 [3], but as we have said, a plethora of different mappings have since been introduced. Here, we want to summarize those which we will explore in this work.

A. Notation, and Majorana and Pauli Operators

It will prove helpful to establish our basic concepts and notation first. The bare fermionic creation and annihilation operators for level p will be denoted as c_p^\dagger and

* thomas.henderson@rice.edu

c_p , respectively, and they interconvert the two fermionic states, via

$$c_p^\dagger |0_p\rangle = |1_p\rangle, \quad (1a)$$

$$c_p |1_p\rangle = |0_p\rangle. \quad (1b)$$

These operators obey canonical anticommutation relations:

$$\{c_p, c_q\} = 0, \quad (2a)$$

$$\{c_p, c_q^\dagger\} = \delta_{pq}, \quad (2b)$$

where $\{A, B\} = AB + BA$ is the anticommutator. The number operator $n_p = c_p^\dagger c_p$ determines whether level p is occupied or empty.

We can draw a close analogy between these fermionic operators and the spin operators. The spin raising and lowering operators, S_p^+ and S_p^- , interconvert the two spin states:

$$S_p^+ |\downarrow_p\rangle = |\uparrow_p\rangle, \quad (3a)$$

$$S_p^- |\uparrow_p\rangle = |\downarrow_p\rangle. \quad (3b)$$

Where the fermionic states $|0_p\rangle$ and $|1_p\rangle$ are eigenstates of the number operator n_p with eigenvalues 0 and 1, respectively, the spin states $|\uparrow_p\rangle$ and $|\downarrow_p\rangle$ are instead eigenstates of the operator S_p^z with respective eigenvalues $+1/2$ and $-1/2$. However, the spin operators obey $\mathfrak{su}(2)$ commutation rules:

$$[S_p^+, S_q^-] = 2 \delta_{pq} S_p^z, \quad (4a)$$

$$[S_p^z, S_q^\pm] = \pm \delta_{pq} S_p^\pm. \quad (4b)$$

We also have the x and y spin operators, which we can obtain from

$$S_p^\pm = S_p^x \pm i S_p^y, \quad (5)$$

which together with S_p^z satisfy

$$[S_p^i, S_q^j] = i \delta_{pq} \epsilon_{ijk} S_p^k, \quad (6)$$

where $i, j, k \in \{x, y, z\}$. Since we are working purely with spin $1/2$, we also have that

$$(S_p^i)^2 = 1/4. \quad (7)$$

While the creation and annihilation operators and the spin operators may be more familiar, they are less convenient for our purposes. Instead, it is easier to use Majorana operators and Pauli operators. We define the Majorana operators $\gamma_{1,p}$ and $\gamma_{2,p}$ as

$$\gamma_{1,p} = c_p + c_p^\dagger, \quad (8a)$$

$$\gamma_{2,p} = i (c_p - c_p^\dagger). \quad (8b)$$

These operators are Hermitian (e.g., $\gamma_{1,p}^\dagger = \gamma_{1,p}$), with $\gamma_{1,p}^2 = \gamma_{2,p}^2 = 1$, and the different Majorana operators all anticommute with one another. Notice that

$$i \gamma_{1,p} \gamma_{2,p} = 1 - 2 n_p. \quad (9)$$

Similarly, we can define Pauli operators, σ_p^i , from

$$S_p^i = \frac{1}{2} \sigma_p^i. \quad (10)$$

Like the Majoranas, the Pauli operators are Hermitian and are involutions ($O^2 = 1$). Paulis on different sites commute, while for Paulis on the same site we may use

$$\sigma_p^i \sigma_p^j = \delta_{ij} 1 + i \epsilon_{ijk} \sigma_p^k. \quad (11)$$

The fact that both Majorana and Pauli operators are Hermitian involutions simplifies converting between fermions and spins; specifically, by taking advantage of the mathematical properties of Pauli and Majorana operators, we reduce the process of finding the inverse transformation to a matrix inversion problem. In practice, having used Pauli and Majorana operators to derive spin to fermion mappings, we must still convert the Hamiltonian from spin operators to Pauli operators (by including appropriate factors of two), then map to Majoranas, and finally convert back to the usual creation and annihilation operators which form the basis of our numerical implementation.

B. The Jordan–Wigner Transformation

Based on the similarities we have noted between the spin operators on the one hand and the fermionic operators on the other, Jordan and Wigner [3] suggested a mapping which, when transforming fermions to spins, we may write as

$$c_p^\dagger \xrightarrow{\text{JW}} S_p^+ \phi_p^z, \quad (12a)$$

$$c_p \xrightarrow{\text{JW}} S_p^- \phi_p^z, \quad (12b)$$

$$\phi_p^z = \prod_{q < p} (-2 S_q^z), \quad (12c)$$

which just means that for states we map

$$|0_p\rangle \xrightarrow{\text{JW}} |\downarrow_p\rangle, \quad (13a)$$

$$|1_p\rangle \xrightarrow{\text{JW}} |\uparrow_p\rangle. \quad (13b)$$

The Hermitian operator ϕ_p^z is the JW string and is responsible for yielding the correct anticommutation relationships. Note that in the quantum computing community, it is common to map $|0_p\rangle$ to $|\uparrow_p\rangle$, which means that the creation operator c_p^\dagger maps to $S_p^- \hat{\phi}_p^z$, where $\hat{\phi}_p^z$ does not have signs in defining the JW strings.

This transformation can be inverted to map spin op-

erators to fermions:

$$S_p^+ \xrightarrow{\text{JW}} c_p^\dagger \tilde{\phi}_p, \quad (14a)$$

$$S_p^- \xrightarrow{\text{JW}} c_p \tilde{\phi}_p, \quad (14b)$$

$$S_p^z \xrightarrow{\text{JW}} n_p - \frac{1}{2}, \quad (14c)$$

$$\tilde{\phi}_p = \prod_{q < p} e^{i\pi n_q} = \prod_{q < p} (1 - 2n_q). \quad (14d)$$

The JW transformation has the virtue of simplicity. Moreover, because it maps the total S^z operator into the total number operator N (modulo an irrelevant shift) it converts fermionic Hamiltonians with number symmetry into spin Hamiltonians with S^z symmetry and vice versa.

We note that the JW transformation depends on the labeling of the sites or fermions, because in the strings for level p we have products over $q < p$. This dependence is of no practical significance if the Hamiltonian is solved exactly, but when mapped Hamiltonians are solved approximately, the result may depend on the ordering of the spins or fermions. One can take advantage of this additional degree of freedom and choose the ordering that minimizes a given cost function, such as the number of Pauli operators in the transformed Hamiltonian [33]. Alternatively, there is an extension of the JW transformation [34] which, at the mean-field level, eliminates this dependency [13].

Finally, we have given the JW transformation in terms of bare fermion and spin operators. Because we find it easier to express the parity transformation in terms of Majorana and Pauli operators, it may be helpful to do the same here. One finds

$$\gamma_{1,p} \xrightarrow{\text{JW}} \sigma_p^x \phi_p^z, \quad (15a)$$

$$\gamma_{2,p} \xrightarrow{\text{JW}} \sigma_p^y \phi_p^z, \quad (15b)$$

$$\phi_p^z = \prod_{q < p} (-\sigma_q^z), \quad (15c)$$

$$\sigma_p^x \xrightarrow{\text{JW}} \gamma_{1,p} \tilde{\phi}_p, \quad (15d)$$

$$\sigma_p^y \xrightarrow{\text{JW}} \gamma_{2,p} \tilde{\phi}_p, \quad (15e)$$

$$\sigma_p^z \xrightarrow{\text{JW}} -i \gamma_{1,p} \gamma_{2,p}, \quad (15f)$$

$$\tilde{\phi}_p = \prod_{q < p} (i \gamma_{1,q} \gamma_{2,q}). \quad (15g)$$

C. The Parity Transformation

The parity (Π) transformation [19] is in some sense the dual companion of the JW transformation. In the JW case, we map the occupation of fermionic level p into the direction of spin p . Because fermions anticommute, occupation numbers alone are not enough to distinguish states, and we must also determine sign information, or parity. In the JW case, the sign information through site

p is found by looking at the occupations of all levels $q < p$. Thus, in JW, *occupation* is encoded locally but *parity* is encoded nonlocally. In contrast, the Π transformation encodes parity information locally, but then must encode occupancy nonlocally.

Specifically, we have

$$\gamma_{1,p} \xrightarrow{\Pi} \psi_p^x \sigma_{p-1}^z, \quad (16a)$$

$$\gamma_{2,p} \xrightarrow{\Pi} -i \psi_p^x \sigma_p^z, \quad (16b)$$

$$\psi_p^x = \prod_{q \geq p} \sigma_q^x. \quad (16c)$$

Inverting this transformation yields

$$\sigma_p^x \xrightarrow{\Pi} i \gamma_{2,p} \gamma_{1,p+1}, \quad (17a)$$

$$\sigma_p^y \xrightarrow{\Pi} i \tilde{\phi}_p \gamma_{1,p} \gamma_{1,p+1}, \quad (17b)$$

$$\sigma_p^z \xrightarrow{\Pi} i \tilde{\phi}_p \gamma_{1,p} \gamma_{2,p}. \quad (17c)$$

With M sites, counting from 1, we must define σ_0^z and $\gamma_{1,M+1}$, which we take to be, respectively,

$$\sigma_0^z \equiv 1, \quad (18a)$$

$$\gamma_{1,M+1} \equiv \Pi = \tilde{\phi}_{M+1} = e^{i\pi N}. \quad (18b)$$

The operator Π is the global number parity operator and acts on number eigenstates to return eigenvalues of ± 1 , depending on whether the state has an even (eigenvalue $+1$) or an odd (eigenvalue -1) number of particles. The presence of this number parity operator leads us to use the symbol Π to refer also to the parity transformation.

Note that the JW transformation singles out the z axis for special treatment, in that σ_p^z is the Pauli operator which does not get a string when it is mapped, while the Π transformation instead singles out the x axis. Of course these choices of axes are merely a matter of convention, and can be rotated arbitrarily. It will be useful to refer to a “rotated parity” transformation which, like the JW mapping, singles out the z axis for special treatment. This rotated Π transformation, denoted by Π_R , just has $\{\sigma_p^x, \sigma_p^y, \sigma_p^z\} \rightarrow \{\sigma_p^z, \sigma_p^x, \sigma_p^y\}$ so that

$$\gamma_{1,p} \xrightarrow{\Pi_R} \psi_p^z \sigma_{p-1}^y, \quad (19a)$$

$$\gamma_{2,p} \xrightarrow{\Pi_R} -i \psi_p^z \sigma_p^y, \quad (19b)$$

$$\psi_p^z = \prod_{q \geq p} \sigma_k^z, \quad (19c)$$

$$\sigma_p^x \xrightarrow{\Pi_R} i \tilde{\phi}_p \gamma_{1,p} \gamma_{1,p+1}, \quad (19d)$$

$$\sigma_p^y \xrightarrow{\Pi_R} i \tilde{\phi}_p \gamma_{1,p} \gamma_{2,p}, \quad (19e)$$

$$\sigma_p^z \xrightarrow{\Pi_R} i \gamma_{2,p} \gamma_{1,p+1}, \quad (19f)$$

$$\sigma_0^y \equiv 1. \quad (19g)$$

Note that the Π transformation converts a single Pauli into a product of two Majoranas, possibly times a string.

Since the string is itself a product of an even number of Majoranas, it seems like the Π transformation should convert each Pauli to a fermionic operator which conserves number parity (since operators which are products of an even number of Majoranas conserve number parity). Unfortunately, at the M^{th} site, we instead have, for the Π transformation, $\sigma_M^x \mapsto i\gamma_{2,M} \Pi$, and this operator changes an even number parity state into an odd number parity state, and vice versa. Something similar happens for σ_M^y . This means that spin Hamiltonians which contain these two operators will typically transform into fermionic Hamiltonians which break number parity symmetry.

D. The Bravyi–Kitaev and Sierpinski Transformations

The JW and Π transformations both use the spin state to represent the information of the occupied orbitals in the corresponding fermionic states, but they do so with a sub-optimal cost due to the need for long strings of Pauli operators to handle occupation changes and phase retrieval. In both cases, evaluating changes in occupation and fermionic phases scales as M , for M spin states. However, we can choose our encoding so that it reduces the lookup and update cost associated with the phase and occupation number of fermionic states. The Bravyi–Kitaev (BK) transformation [14, 19] achieves this goal with $\mathcal{O}(\log_2(M))$ scaling in the following way.

The BK transformation improves the encoding efficiency by iteratively bisecting sets of fermionic modes to store partial sums in spin states. This approach enables efficient parity checks for any set of modes while minimizing the number of spins that need to be flipped during raising or lowering operations [35]. The transformation is captured by a matrix β_M^{BK} , which linearly maps Fock basis states $|f\rangle$ to encoded spin states $|\sigma\rangle^{\text{BK}}$ using addition modulo 2. This matrix is illustrated below for $M = 8$:

$$|\sigma\rangle^{\text{BK}} \equiv \beta_M^{\text{BK}} |f\rangle := \begin{pmatrix} 1 & & & & & & & \\ 1 & 1 & & & & & & \\ & & 1 & & & & & \\ 1 & 1 & 1 & 1 & & & & \\ & & & & 1 & & & \\ & & & & & 1 & 1 & \\ & & & & & & & 1 \\ 1 & 1 & 1 & 1 & 1 & 1 & 1 & 1 \end{pmatrix} \begin{pmatrix} n_1 \\ n_2 \\ n_3 \\ n_4 \\ n_5 \\ n_6 \\ n_7 \\ n_8 \end{pmatrix}, \quad (20)$$

resulting in

$$\begin{pmatrix} \sigma_1 \\ \sigma_2 \\ \sigma_3 \\ \sigma_4 \\ \sigma_5 \\ \sigma_6 \\ \sigma_7 \\ \sigma_8 \end{pmatrix} = \begin{pmatrix} n_1 \\ n_1 + n_2 \\ n_3 \\ n_1 + n_2 + n_3 + n_4 \\ n_5 \\ n_5 + n_6 \\ n_7 \\ n_1 + n_2 + n_3 + n_4 + n_5 + n_6 + n_7 + n_8 \end{pmatrix}. \quad (21)$$

All the information needed to replicate the group action of the fermionic raising and lowering operators is accessible from these spins. For each mode i , there are three sets of spin indices to consider. The Update set $U(i)$, comprises the spin sites needed to flip if the occupation of fermionic mode i is changed. The Parity set $P(i)$, the minimum set of spins required to compute the parity of fermionic modes up to $i - 1$. The Flip set $F(i)$, i.e., the smallest set of additional spin states needed to determine whether the i th spin state is equal to the i th fermionic occupation number or its opposite. For ease of notation, an operator with the subscript set \mathcal{S} will be taken to mean “the tensor product of this operator on each element in \mathcal{S} ” where appropriate; e.g., $(\sigma^z)_{\mathcal{S}} = \prod_{s \in \mathcal{S}} (\sigma^z)_s$.

To know whether to associate c_i^\dagger with S_i^+ or S_i^- , consider the projection operators onto spaces of even or odd parity over a set \mathcal{S} :

$$E_{\mathcal{S}} = \frac{1}{2}(I + (\sigma^z)_{\mathcal{S}}) \quad O_{\mathcal{S}} = \frac{1}{2}(I - (\sigma^z)_{\mathcal{S}}) \quad (22)$$

and incorporate the knowledge from the Flip set to guarantee that the correct association is made with the new BK spin raising and lowering operators:

$$\begin{aligned} \Pi_i^+ &= S_i^+ \otimes E_{F(i)} - S_i^- \otimes O_{F(i)} \\ &= \frac{1}{2} ((\sigma^x)_i \otimes (\sigma^z)_{F(i)} - (i\sigma^y)_i) \\ \Pi_i^- &= S_i^- \otimes E_{F(i)} - S_i^+ \otimes O_{F(i)} \\ &= \frac{1}{2} ((\sigma^x)_i \otimes (\sigma^z)_{F(i)} + (i\sigma^y)_i) \end{aligned} \quad (23)$$

Finally, with properly constructed BK spin raising and lowering operators, and Update, Parity, and Flip sets, it is possible to define the fermionic creation and annihilation operators, as

$$\begin{aligned} c_i^\dagger &\xrightarrow{\text{BK}} (\sigma^z)_{P(i)} \otimes (\sigma^x)_{U(i)} \otimes \Pi_i^+, \\ c_i &\xrightarrow{\text{BK}} (\sigma^z)_{P(i)} \otimes (\sigma^x)_{U(i)} \otimes \Pi_i^-. \end{aligned} \quad (24)$$

This formalism is completely generic. The only thing that determines the representation of the encoding is the occupation storage matrix β_M . For JW, this is the identity matrix, while for the Π transformation, it is the lower-diagonal matrix with all 1s.

The bisections in the construction of the BK encoding matrix β_M^{BK} ensure $\mathcal{O}(\log_2(M))$ scaling for all three

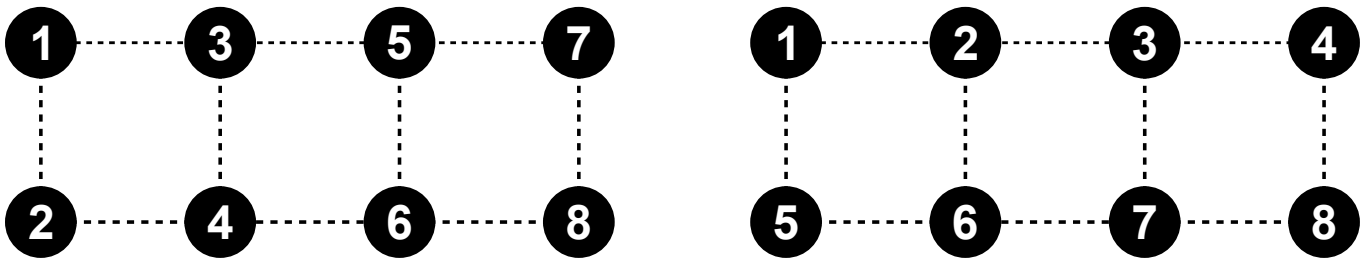


FIG. 1. Labeling schemes for quasi-1D lattices. Left: the “ $2 \times n$ ” labeling for $n = 4$. Right: the “ $n \times 2$ ” labeling for $n = 4$.

vacuum:

$$|\Phi_{\text{HFB}}\rangle = e^Z |-\rangle = \mathcal{N} e^{\mathcal{T}} |-\rangle, \quad (32a)$$

$$Z = \sum_{p < q} (Z_{pq} c_p^\dagger c_q^\dagger - h.c.), \quad (32b)$$

$$\mathcal{T} = \sum_{p < q} \mathcal{T}_{pq} c_p^\dagger c_q^\dagger. \quad (32c)$$

In addition to its use in number-conserving Hamiltonians, HFB is also the natural mean-field for fermionic Hamiltonians which lack number symmetry but have number parity symmetry. The number parity operator is a symmetry of, so far as we are aware, all physical fermionic Hamiltonians. Frequently, however, it is not a symmetry of spin Hamiltonians which have been transformed to fermions. When the number parity operator is not a symmetry of the fermionic Hamiltonian, we must step beyond more standard mean-field theories [32]. One approach, pioneered by Colpa [38], is the addition of a single extra fermionic degree of freedom, not used in the Hamiltonian but present in the Hilbert space, which permits us to then use standard HFB. Alternatively, we can use a mean-field directly constructed for these parity-violating Hamiltonians. We call this mean-field HFBF [29–32, 39] and it is defined in analogy to HF and HFB. We can use a canonical transformation with a nonlinear component to define quasiparticle creation and annihilation operators, with a unitary transformation matrix. We can instead choose a Thouless parameterization, as we will prefer to do here, writing

$$|\Phi_{\text{HFBF}}\rangle = \mathcal{N} (1 + t) e^{\mathcal{T}} |-\rangle, \quad (33a)$$

$$t = \sum_p t_p c_p^\dagger, \quad (33b)$$

or using an equivalent unitary form.

As a practical matter, for both HFB and HFBF, we use as a reference not the physical vacuum $|-\rangle$ but some well-chosen reference $|\Phi_0\rangle$, just as we do for HF. In this case, we employ a quasiparticle transformation so that \mathcal{T} and t are excitation operators acting on $|\Phi_0\rangle$:

$$\mathcal{T} = \sum_{i < j} \mathcal{T}_{ij} c_i c_j + \sum_{ia} \mathcal{T}_{ai} c_a^\dagger c_i + \sum_{a < b} \mathcal{T}_{ab} c_a^\dagger c_b^\dagger, \quad (34a)$$

$$t = \sum_i t_i c_i + \sum_a t_a c_a^\dagger, \quad (34b)$$

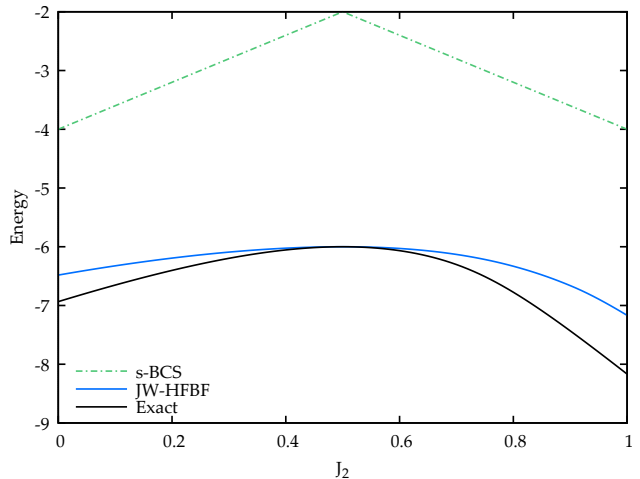


FIG. 2. Total energies in the 2×4 J_1 - J_2 model with periodic boundary conditions. We compare the spin mean-field (“s-BCS”) and the fermionic mean-field in the Jordan-Wigner-transformed Hamiltonian (“JW-HFBF”) to the results of exact diagonalization (“Exact”).

where i and j (a and b) index levels occupied (empty) in $|\Phi_0\rangle$. Note that in making this quasiparticle transformation, we use bare fermion annihilation operators for the levels occupied in $|\Phi_0\rangle$ rather than creation operators.

Although the various mean-field methods we need can be implemented in a self-consistent field code with polynomial scaling, we have chosen instead for simplicity to implement all of them in a full configuration interaction code, using the conjugate gradient algorithm to minimize the mean-field energy with respect to the Thouless parameters. We have chosen a non-unitary Thouless representation, for which the analytic gradient of the wave function and energy is straightforward. Implementing these various techniques in an exact diagonalization scheme facilitates comparison between the various fermionizations, as we can implement each spin operator in a straightforward way, whereas in a self-consistent field code we would require either high-order density matrices or the use of a nonorthogonal version of Wick’s theorem [40, 41]. Unfortunately, this choice limits us to about a dozen sites for practical calculations.

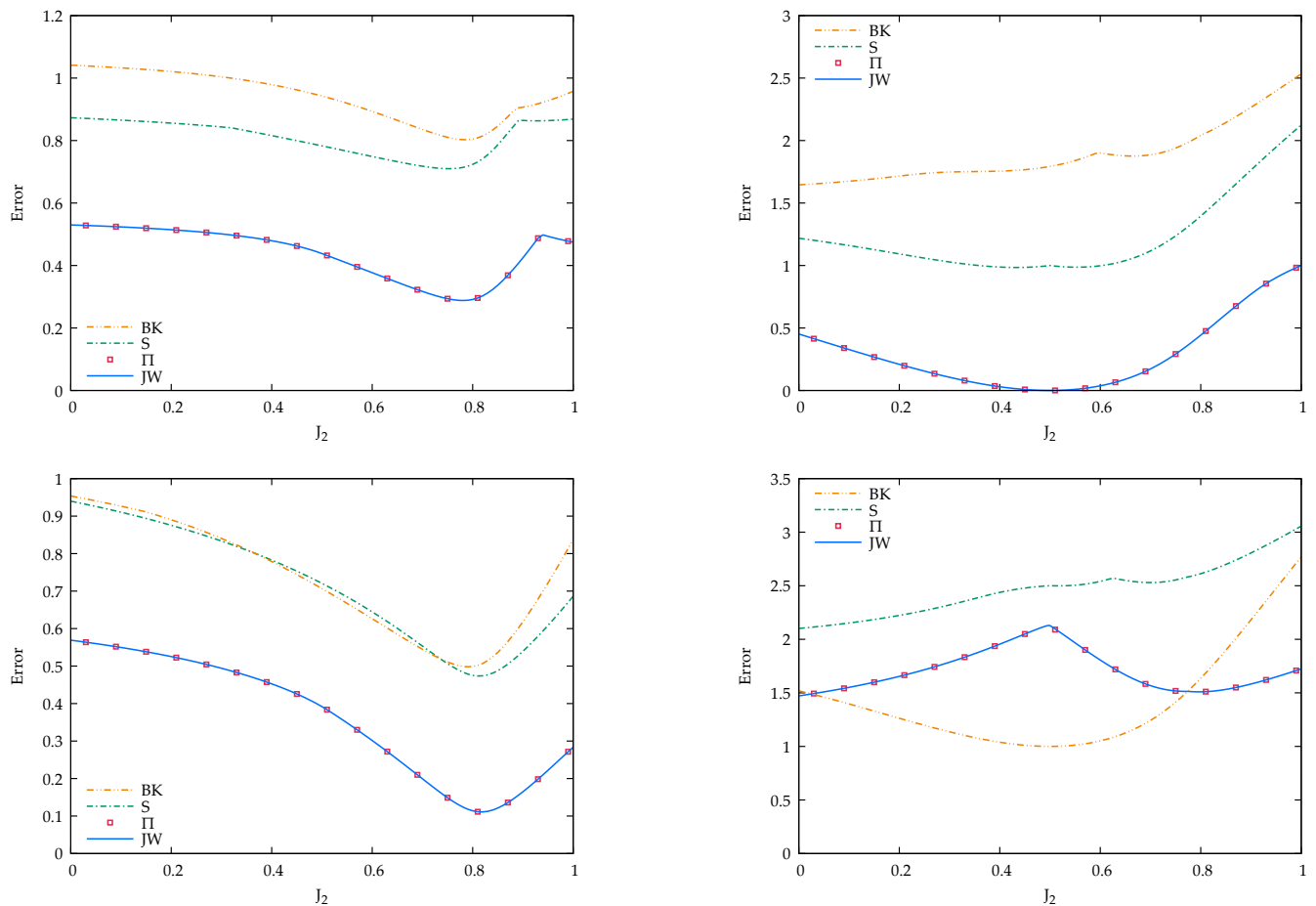


FIG. 3. HFBF mean-field energy errors relative to the exact diagonalizations in the fermionized 2×4 J_1 - J_2 model with $J_1 = 1$ and either open boundary conditions (OBC) or periodic boundary conditions (PBC). Top left: 2×4 labeling with OBC. Top right: 2×4 labeling with PBC. Bottom left: 4×2 labeling with OBC. Bottom right: 4×2 labeling with PBC.

IV. RESULTS

Now that we have outlined the various fermionizations we will consider and have touched on the mean-field methods we will employ, we can proceed to analyze the various techniques. With the exception of the JW transformation, the fermionizations map spin Hamiltonians which possess S_z symmetry onto fermionic Hamiltonians which have neither number symmetry nor number parity symmetry, so we must use the general HFBF mean-field. In contrast, for JW the transformed Hamiltonian has number symmetry; this means that in the JW case we may try HF and HFB in addition to HFBF. To eliminate one variable from consideration, we will use HFBF for the JW-transformed Hamiltonian as well, except when indicated otherwise. Generally, however, we find that for the JW-transformed Hamiltonian, number parity symmetry does not spontaneously break at the mean-field level so that HFBF and HFB are entirely equivalent.

In this work, we will consider three $\mathfrak{su}(2)$ Hamiltonians: the J_1 - J_2 Heisenberg model, the spin XXZ model,

and the pairing Hamiltonian which we write in terms of spin operators. We will discuss results for each in turn. The two Heisenberg Hamiltonians are commonly studied textbook models (see, for example, Ref. 42); although they can be used to model certain physical systems [43–45], their practical utility is as simple models which exhibit spin frustration. The pairing Hamiltonian essentially models Bardeen-Cooper-Schrieffer (BCS) [46] superconductivity (and is also known as the reduced BCS Hamiltonian), but has also been used to describe, for example, ultrasmall superconducting grains [47]. All of these Hamiltonians have S_z symmetry, and we will always work in the $S_z = 0$ sector for simplicity. In the parameter regimes we will consider, this is always the global ground state. In the thermodynamic limit, these Hamiltonians exhibit phase transitions which are of course absent in the exact solution for the finite systems we will consider here. Nevertheless, the presence of these multiple spin arrangements is reflected in mean-field solutions which frequently just cross one another. This leads to error curves which are not entirely smooth, because we have

plotted, at each Hamiltonian parameter value, the lowest energy mean-field solution we could find.

Because our results depend on the labeling scheme chosen, we must say a bit about this first. In one dimension, we use the natural labeling scheme where sites connected in the lattice have sequential numbers, e.g., site 1 connects to site 2, site 2 to site 3, and so on. For the quasi-1D spin ladders, however, we have a “ $2 \times n$ ” labeling scheme and a “ $n \times 2$ ” labeling scheme, depicted in Fig. 1. Put simply, the first number (“2” or “ n ”) denotes the faster-moving index in the 2D lattice.

A. The J_1 - J_2 Hamiltonian

The J_1 - J_2 model has both nearest-neighbor and next-nearest neighbor interactions:

$$H_{J_1-J_2} = J_1 \sum_{\langle pq \rangle} \vec{S}_p \cdot \vec{S}_q + J_2 \sum_{\langle\langle pq \rangle\rangle} \vec{S}_p \cdot \vec{S}_q, \quad (35)$$

where $\langle pq \rangle$ denotes nearest neighbors (sites connected in the lattice) and $\langle\langle pq \rangle\rangle$ denotes next-nearest neighbors. The physics is driven by the ratio J_2/J_1 , where we will take both to be positive. For the 2D square lattice in the thermodynamic limit, the ground state is a Néel antiferromagnet for $J_2 \lesssim 0.4 J_1$ and a striped antiferromagnet for $J_2 \gtrsim 0.6 J_1$. In between, the magnetic structure is more complicated [48–50]. In this work we will focus on the quasi-1D spin ladders, i.e., $2 \times n$ systems.

As we have shown elsewhere [12], results using mean-field theory in combination with the JW transformation are not quantitative but are greatly superior to what one obtains with an $\mathfrak{su}(2)$ mean-field technique, being roughly comparable to configuration interaction with double and quadruple excitations atop the symmetry-adapted spin mean-field. To get some sense of the difference in quality between fermionic mean-field and $\mathfrak{su}(2)$ mean-field, Fig. 2 compares total energies from the spin and fermionic mean-fields to the exact results for the 2×4 model.

Figure 3 shows a comparison of the total energy errors with respect to the exact diagonalizations, resulting from the mean-field solutions with the four different fermionization schemes, both for open boundary conditions (OBC) and periodic boundary conditions (PBC), with $J_1 = 1$. We can immediately see that the JW and Π transformations give completely identical mean-field energies, which is sensible since, as we have noted, these two transformations are loosely speaking dual companions of one another. More formally, as we will discuss in future publications, the JW-transformed fermionic operators of Eqn. 15 and the Π_R -transformed operators of Eqn. 19 are, themselves, related by a mean-field canonical transformation of a form equivalent to HFBF; accordingly, the two seemingly different Hamiltonians have identical mean-field solutions.

The BK and Sierpinski mappings generally yield significantly worse mean-field results than do the other trans-

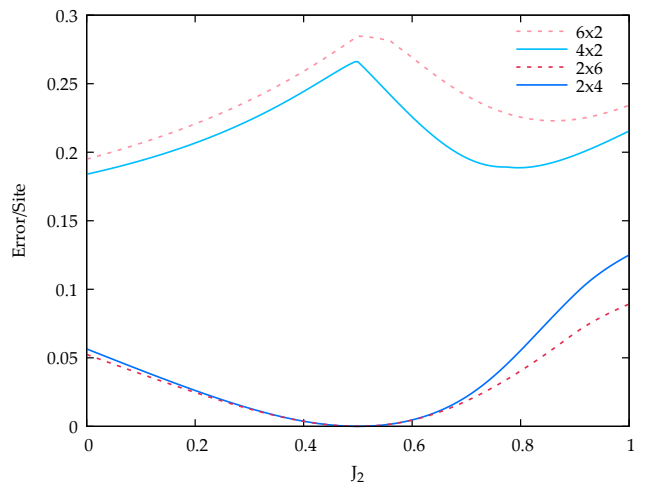


FIG. 4. HFBF mean-field energy errors per site relative to the exact diagonalization in the 2×4 and 2×6 JW-transformed J_1 - J_2 Hamiltonian.

formations we have considered. Mappings designed to minimize gate depth when mapping fermions to spins are not, evidently, the same as mappings designed to yield optimal mean-field solutions when mapping spins to fermions. The one apparent exception is in the 4×2 case with PBC, where the BK mapping is, overall, superior in the physically interesting regime around $J_2 = 1/2$.

We also see the expected dependence on the labeling scheme, which we recall can be eliminated in the JW case (and, presumably, in the Π case) by generalizing the strings $\tilde{\phi}_p$. It is interesting to note that we generally obtain superior results for OBC with the 4×2 labeling and for PBC with the 2×4 labeling where JW and Π are exact at $J_2 = 1/2$, presumably related to the Majumdar-Ghosh point in the 1D J_1 - J_2 model where the ground state at $J_2 = 1/2$ is exactly dimerized [51].

Finally, we compare results for the 2×4 and 2×6 models in Fig. 4. These results (consistent with those of Ref. 13) suggest that increasing system size does not necessarily degrade the quality of the mean-field results. In other words, as is the usual case for mean-field theory, our results are extensive; see also the supplementary material.

B. The XXZ Hamiltonian

The XXZ Hamiltonian is also a spin lattice model, this time given by

$$H_{\text{XXZ}} = \sum_{\langle pq \rangle} (S_p^x S_q^x + S_p^y S_q^y + \Delta S_p^z S_q^z). \quad (36)$$

Where the physics of the J_1 - J_2 model depends on J_2/J_1 , here it depends on Δ . In one dimension, at $\Delta = 0$ the JW-transformed XXZ model is exactly solved by HF with

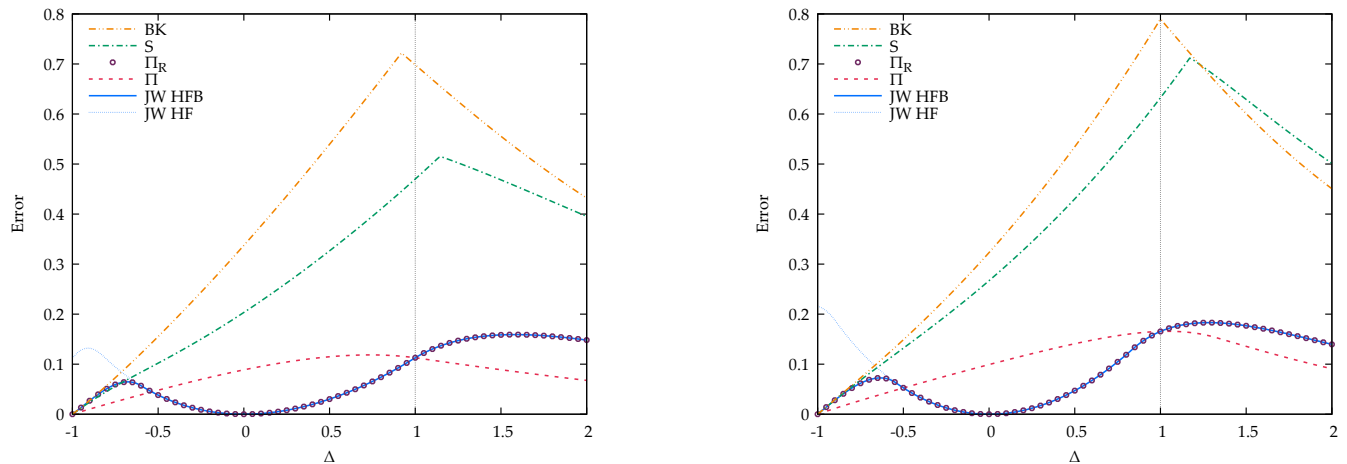


FIG. 5. HFBF (BK, Sierpinski, Π_R , Π) and HF and HFB (JW) mean-field energy errors relative to the exact diagonalizations in the fermionized 8-site 1D XXZ model. Left panel: OBC. Right panel: PBC.

sites labeled in a natural sequential way. This is not the case in two or more dimensions, so we will consider both the 1D system and the 2D rectangular lattice. The point at $\Delta = 1$ is the Heisenberg point, at which the Hamiltonian has S^2 symmetry, while $\Delta = -1$ is also a special point in which the exact ground state is given by the extreme antisymmetrized geminal power [52, 53].

The ground state over all S_z sectors occurs at $S_z = 0$ for $\Delta > -1$, while the different S_z sectors are all degenerate with one another at $\Delta = -1$ and the global minimum of the energy occurs at maximal S_z for $\Delta < -1$. Since we are focusing on $S_z = 0$ we will only consider $\Delta \geq -1$ in this work. In the thermodynamic limit, for rectangular lattices, there is a phase transition at $\Delta = 1$, where for $\Delta > 1$ the ground state is antiferromagnetic with magnetization along the z axis and for $|\Delta| < 1$ the ground state is instead magnetized in the xy plane [54].

We begin with the 1D case, depicted in Fig. 5, in which the JW strings do not contribute. Again, the Π and JW transformations provide uniformly more accurate results than we obtain with the other two mappings considered, although all methods are exact at $\Delta = -1$ where, as we have indicated, the ground state energy for each S_z sector is the same and spin mean field is already exact. As expected, we get the exact result at $\Delta = 0$ with the JW transformation.

Unlike with the J_1 - J_2 model, the JW and Π transformations do not generally give the same result, except at $\Delta = \pm 1$. At $\Delta = 1$ the XXZ model is isotropic, but elsewhere it treats the z component of spin differently from the other two. For this reason, we also show the Π_R transformation which, like JW and like the Hamiltonian, treats the z component of spin differently (because it does not include the string operator $\tilde{\phi}_p$). Indeed, the Π_R transformation yields results completely equivalent to those we obtain with JW. We have also verified that a rotated JW transformation which has strings for the y and z spin components but not the x component yields

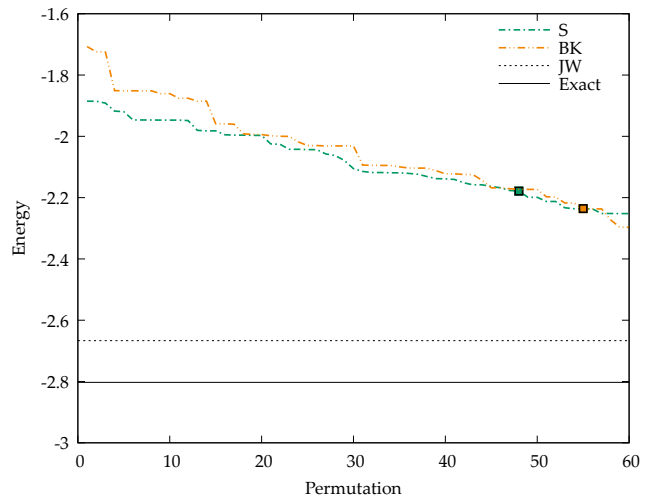


FIG. 6. HFBF mean-field energy for the unique labelings of the 6-site 1D XXZ model at $\Delta = 1$ with PBC, based on the BK and Sierpinski encodings. The lines marked “JW” and “Exact” denote, respectively, the energy of the mean-field solution based on the JW transformation with the natural labeling scheme 1-2-3-4-5-6, and the exact ground state energy. The squares indicate the result based on the natural labeling scheme.

results identical to the original Π transformation (data not shown).

We must mention one other consideration. For most Δ values, the fermionic mean-field for the JW-transformed Hamiltonian is HF. Near $\Delta = -1$, however, number symmetry breaks spontaneously and we can distinguish HF and HFB solutions. Where these two methods differ, it is the lower energy of the two (the HFB) with which the HFBF solution for the Π_R transformation agrees.

One may wonder whether the poor performance of the BK or Sierpinski encodings in this context is simply due

to having chosen the wrong labeling scheme. We have seen that labeling schemes matter for all of these encodings, and previous work has found that the natural labeling scheme we have chosen is, on the whole, the best available for the 1D XXZ model with the JW transformation. But is that the case for these encodings?

To answer that question, we have looked at the 6-site 1D XXZ model with PBC. Here, there are 60 distinct labeling schemes (6! ways of labeling the sites, reduced by a factor of 6 due to translational symmetry and by another factor of 2 due to reflection symmetry) and we have tried the BK and Sierpinski encodings at $\Delta = 1$ for all 60 distinct labelings. The results in Fig. 6 make clear that no relabeling of the sites will suffice to remedy the poor performance of mean-field methods based on these encodings, at least at $\Delta = 1$ but presumably also for other values of Δ .

Results for the 2D XXZ model are roughly similar to those for the 1D case (see Fig. 7) although the mean-field methods are generally less accurate. For the JW and Π transformations, this is presumably because the strings $\tilde{\phi}_p$ which vanished in 1D now contribute in 2D. The BK and Sierpinski encodings are more competitive with the JW and Π encodings in this quasi-1D case than they are in the genuinely 1D case, but the JW and Π encodings still generally appear to yield superior mean-field results.

C. The Pairing Hamiltonian

The pairing Hamiltonian, also known as the reduced Bardeen–Cooper–Schrieffer Hamiltonian, is not really a Hamiltonian of spins at all. Instead, it is a Hamiltonian consisting of electron pair creation, pair annihilation, and number operators. As these operators satisfy the same $\mathfrak{su}(2)$ algebra as do the spin operators, however, we can write the pairing model as a spin Hamiltonian, in which case it takes the form

$$H_P = \sum_p \epsilon_p (2S_p^z - 1) - G \sum_{pq} S_p^+ S_q^+. \quad (37)$$

This Hamiltonian is exactly solvable with a form of Bethe ansatz [55–57], for any choice of ϵ_p and G .

We can eliminate the $p = q$ term in the interaction, using $S_p^+ S_p^- = \frac{1}{2} + S_p^z$, thereby absorbing this diagonal contribution into the first, Zeeman-like, term. As a practical matter, we choose to work at half filling, in which case we can rewrite the Hamiltonian as

$$H'_P = 2 \sum_p \epsilon_p S_p^z - G \sum_{p \neq q} S_p^+ S_q^+ = H_P - \lambda S_z \quad (38)$$

and pick the ϵ to be equally spaced and centered around 0. The chemical potential λ enforces that the ground state is $S_z = 0$ everywhere, and the physics is driven by the parameter G .

If we disregard the chemical potential for a moment and consider only the first form of the Hamiltonian, we

can see that as $|G|$ tends to ∞ , so that the Zeeman-like term is irrelevant, then

$$\frac{1}{|G|} H_P \rightarrow \mp S_+ S_- = \mp (S^2 - S_z^2 + S_z), \quad (39)$$

where $S_+ = \sum_p S_p^+$ and similarly for S_- and S_z ; the sign is \mp as $G \rightarrow \pm\infty$. Accordingly, the $S_z = 0$ ground state occurs for maximal S^2 in the $G \rightarrow \infty$ limit and for $S^2 = 0$ in the $G \rightarrow -\infty$ limit. Respectively, these amount to an extreme form of the antisymmetrized geminal power, and a kind of dimerized state obtained by taking one of the (many) degenerate $S^2 = 0$ states. See Refs. 58–60 for details.

The pairing model presents a particular challenge. Where in the 2D XXZ models, each spin interacted with at most three other spins, in the pairing model, each spin interacts equivalently with *every* other spin. Indeed, Fig. 8 shows that for the pairing model, our results are generally rather poor away from $G = 0$, though again the JW and (rotated) Π transformations are superior to the other fermionizations on the repulsive side ($G < 0$).

D. Fermionic Number Projection

For most of these fermionizations, we have gone about as far as we can go with mean-field theory. For the JW transformation, however, we can do a bit better. This is because the JW transformation maps the global S_z symmetry of the $\mathfrak{su}(2)$ Hamiltonian to global number symmetry of the fermionic Hamiltonian, and we can deliberately break and then projectively restore this number symmetry to do a JW-transformed number-projected HFB. For details about number projection, see Refs. 61–63, but the gist is that we write the projected HFB (PHFB) wave function as an HFB state and then project out those components with the incorrect particle number. We could do something analogous for any of the other encodings – the global S_z symmetry maps under all of them to *some* symmetry of the fermionic Hamiltonian – but JW has the advantage that this symmetry is both obvious and, more importantly, given by a one-body operator. As such, the projection can be efficiently implemented in a self-consistent field code.

Fortunately, PHFB provides quite reasonable accuracy for the JW-transformed pairing Hamiltonian, as seen in Fig. 9. In fact, it is energetically exact in both the strongly attractive ($G \rightarrow \infty$) and strongly repulsive ($G \rightarrow -\infty$) limits. We prove this in the appendix.

Figure 10 shows that PHFB is also a useful improvement upon HF or HFB in the JW-transformed XXZ model. Indeed, PHFB is variationally bounded from above by HFB (at least when we are looking at the ground state number sector), so it must be at least as good as the results we obtained for the J_1 – J_2 and XXZ models with HFB on the JW-transformed Hamiltonian.

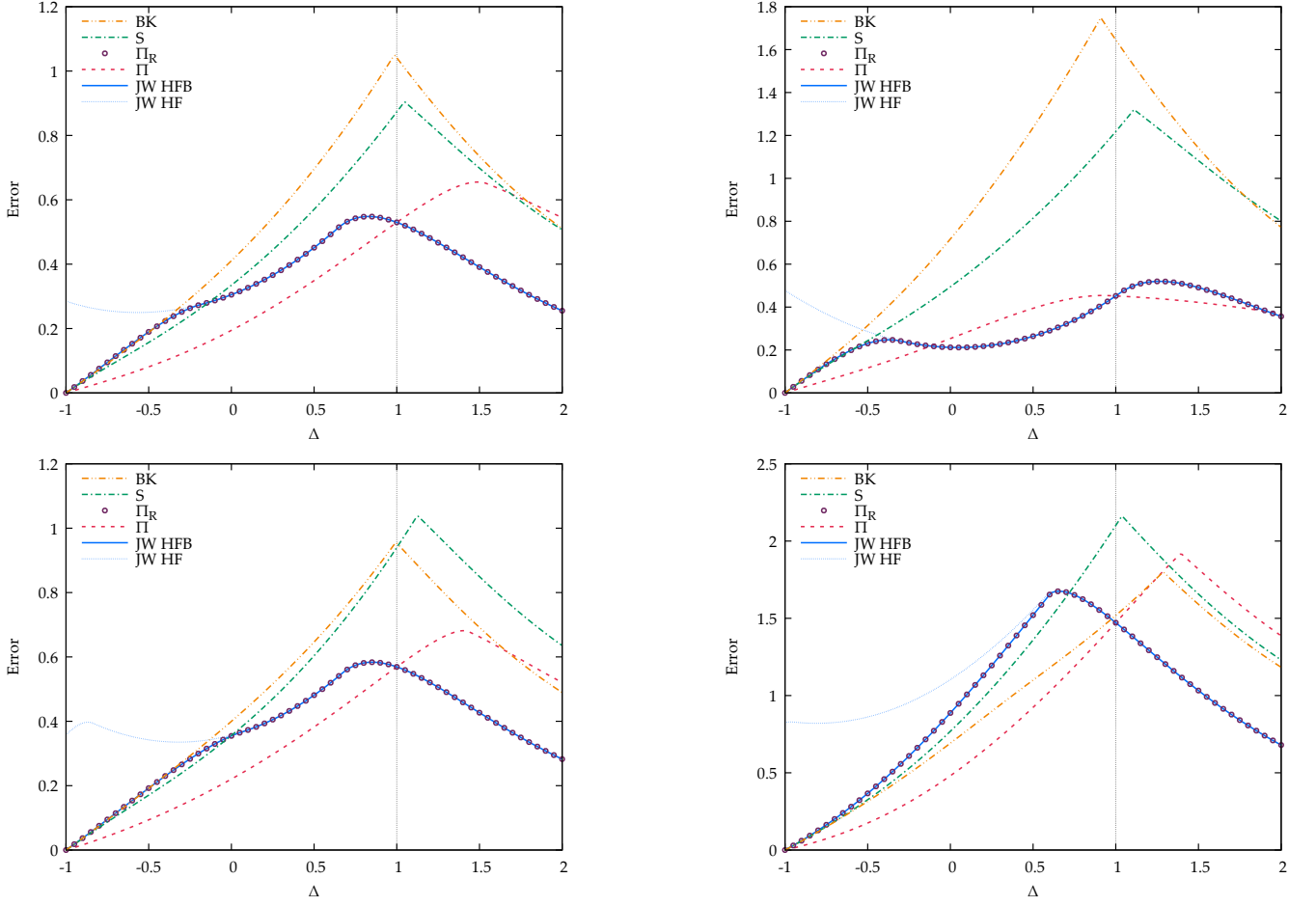


FIG. 7. HFBF (BK, Sierpinski, Π_R , Π) and HF and HFB (JW) mean-field energy errors relative to the exact diagonalizations in the fermionized 2×4 XXZ model with either open boundary conditions (OBC) or periodic boundary conditions (PBC). Top left: 2×4 labeling with OBC. Top right: 2×4 labeling with PBC. Bottom left: 4×2 labeling with OBC. Bottom right: 4×2 labeling with PBC.

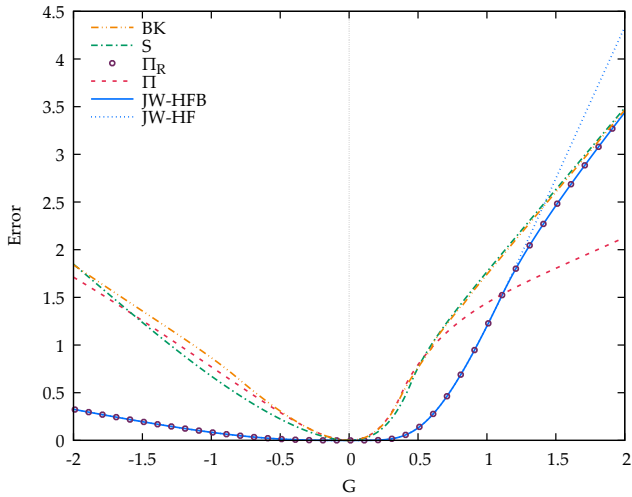


FIG. 8. HFBF (BK, Sierpinski, Π_R , Π) and HF and HFB (JW) mean-field energy errors relative to the exact diagonalizations in the fermionized 8-site pairing model.

V. DISCUSSION

Each of the fermionizations we have considered preserves the exact spectrum of the spin Hamiltonian, but they generally give different results at the mean-field level. In other words, all fermionizations are equivalent in the full Fock space, but some fermionizations are more compatible with mean-field approaches than others. For the Hamiltonians we have considered, those fermion to $\mathfrak{su}(2)$ mappings designed to produce more efficient encodings seem to yield fermionic Hamiltonians whose mean-field solutions are energetically less accurate. This is so even though the JW or Π transformations involve the very nonlocal JW strings $\tilde{\phi}_p$, which the BK and Sierpinski encodings eliminate. Fortunately, the action of the JW string on a fermionic mean-field state is to produce another mean-field state by virtue of the Thouless theorem [36]. This means that it is actually straightforward to account for the JW strings when evaluating matrix elements, by simply using the non-orthogonal Wick's the-

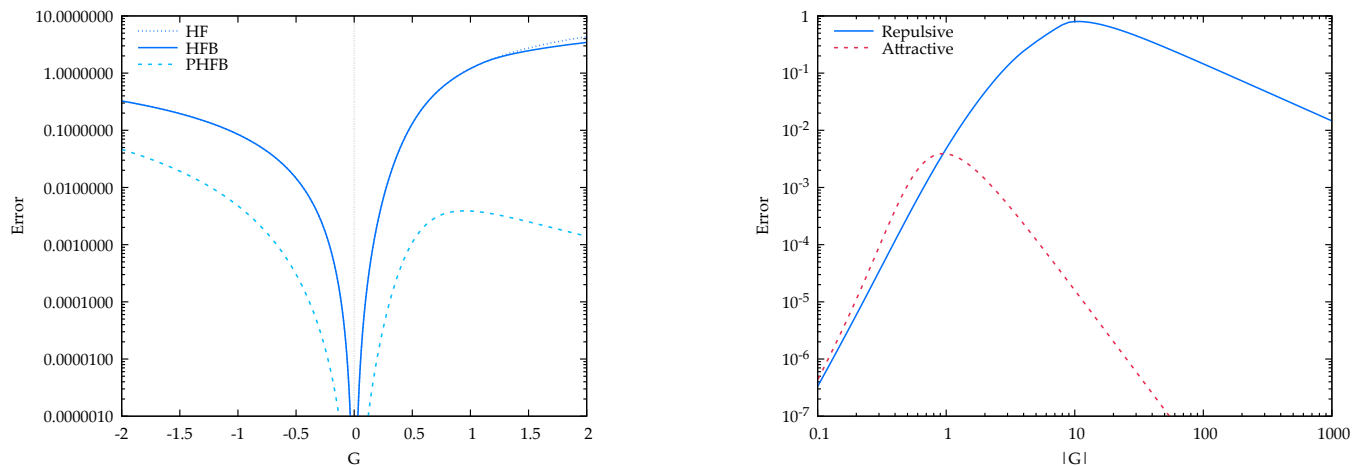


FIG. 9. Mean-field energy errors relative to the exact diagonalizations in the 8-site pairing model transformed with JW. Left panel: Comparison between HF, HFB, and PHFB. Right panel: PHFB errors on a log-log scale to show the large $|G|$ behavior.

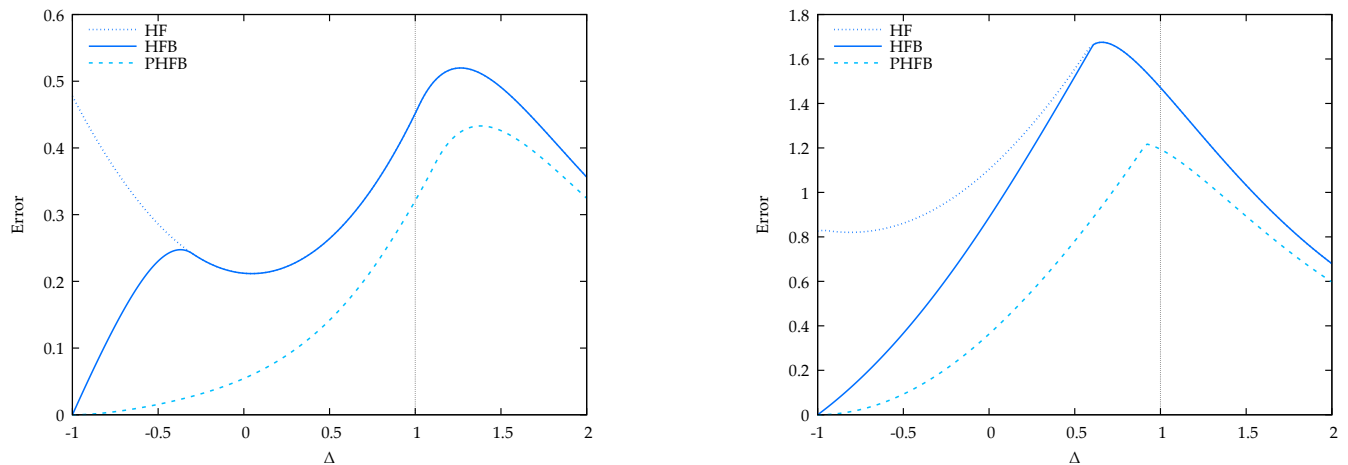


FIG. 10. Energy errors relative to the exact diagonalizations in the 2×4 JW-transformed XXZ model with PBC for HF, HFB, and PHFB. Left panel: 2×4 labeling. Right panel: 4×2 labeling.

orem [40], though some care must be taken to implement this idea in a numerically robust and efficient way [41].

Another advantage of the JW transformation is that by generalizing the string from $\tilde{\phi}_p = \exp(i\pi \sum_{q<p} n_q)$ to

$$\hat{\phi}_p = e^{i \sum_q \theta_{qp} n_q} \tilde{\phi}_p \quad (40)$$

where the matrix of parameters θ is symmetric with vanishing diagonals, we can obtain results invariant to the labeling of the spin lattice [13] when θ is optimized. This generalization, too, can be readily implemented using nonorthogonal Wick's theorem. The same should be true for the Π transformation.

There is one additional advantage which suggests we should prefer to use the JW transformation to the Π mapping: the JW mapping converts an $\mathfrak{su}(2)$ Hamiltonian with S_z symmetry to a fermionic Hamiltonian with number symmetry. This permits us to select several different

levels of mean-field theory: HF, HFB, HFBF, as well as their number-projected counterparts. The other mappings all require us to use the rather more complicated HFBF mean-field theory or to employ Colpa's trick to replace HFBF for M fermions with HFB for $M+1$ fermions (and the latter is pragmatically simpler) and generally do not permit symmetry projection at all. This is not to say that these fermionized Hamiltonians do not inherit the symmetries of the underlying spin Hamiltonian, because naturally they do. Rather, these symmetries are not generally one-body symmetries and therefore are difficult to project efficiently.

For all of these reasons, it seems clear that the JW transformation, in addition to being the oldest mapping relating spins to fermions, is (in the context of mapping spin Hamiltonians to fermions for mean-field solution) also the most powerful (at least among those we have tried).

SUPPLEMENTARY MATERIAL

See supplementary material for the proof that spin mean-field maps, under Jordan-Wigner transformation, to a special case of the fermionic HFBF mean-field. We also provide additional numerical evidence of the extensivity of our results.

ACKNOWLEDGMENTS

This work was supported by the U.S. Department of Energy, Office of Basic Energy Sciences, under Award DE-SC0019374. G.E.S. is a Welch Foundation Chair (C-0036). JDW holds concurrent appointments at Dartmouth College and as an Amazon Visiting Academic. This paper describes work performed at Dartmouth College and is not associated with Amazon.

Appendix A: Exactness of JW-PHFB for the Pairing Model

Here we demonstrate exactness of number-projected HFB in the $G \rightarrow \pm\infty$ limit of the JW-transformed pairing model. As we have noted, in the $S_z = 0$ sector we can work with the simpler Hamiltonian

$$H_{\text{eff}} = \mp S^2; \quad (\text{A1})$$

see Eqn. 39.

Let us start with the attractive limit. In this case, we know that the ground state we seek has $S_z = 0$ and maximal S^2 . We can build this by starting with the state with all spins \downarrow and applying the global raising operator the appropriate number of times to reach

$$|\Psi_A\rangle = \frac{1}{N!} \left(\sum_p S_p^+ \right)^N |\downarrow\rangle = P_{S_z} e^{\sum_p S_p^+} |\downarrow\rangle \quad (\text{A2})$$

where N is the number of \uparrow spins and $|\downarrow\rangle$ is the vacuum in which each spin is \downarrow ; P_{S_z} is the projector onto the appropriate S_z sector. The wave function $\exp(\sum_p S_p^+) |\downarrow\rangle$ is a spin mean-field state.

Now transform this wave function with the JW transformation. Because S_z becomes particle number, P_{S_z} transforms to the fermionic number projector. We have argued elsewhere [32] (and prove in the supplementary material) that a spin mean-field state maps into a fermionic HFBF state, which means that $|\Psi_A\rangle$ maps, under JW transformation, into a number-projected HFBF state. But a number-projected HFBF state is also a number-projected HFB state since HFBF is just a linear combination of an even-particle number HFB and an odd-particle number HFB. Ergo, the exact ground state in the $G \rightarrow \infty$ limit of the pairing model maps, under JW, into PHFB.

The repulsive limit is more complicated. As we have noted, it is an $S^2 = 0$ state, which we can get by the standard machinery of coupling angular momenta. One way to write (one of) the ground states is in a dimerized form:

$$|\Psi_R\rangle = |s_{12}\rangle \otimes |s_{34}\rangle \dots |s_{M-1,M}\rangle, \quad (\text{A3a})$$

$$|s_{pq}\rangle = |\uparrow_p \downarrow_q\rangle - |\downarrow_p \uparrow_q\rangle, \quad (\text{A3b})$$

where we have a total of M spins. That is, we divide the system into disjoint pairs and place each pair in a separate singlet state. We can express this wave function as

$$|\Psi_R\rangle = \left[\prod_{k=1}^{M/2} (1 - S_{2k}^+ S_{2k-1}^-) \right] |\uparrow\downarrow\uparrow\downarrow\dots\rangle. \quad (\text{A4})$$

Now we transform the wave function with the JW transformation. The state $|\uparrow\downarrow\uparrow\downarrow\dots\rangle$ becomes a fermionic state $|1010\dots\rangle$ with odd levels occupied and even levels empty. The operator $S_{2k}^+ S_{2k-1}^-$ transforms as

$$S_{2k}^+ S_{2k-1}^- \xrightarrow{\text{JW}} c_{2k}^\dagger \tilde{\phi}_{2k} \tilde{\phi}_{2k-1} c_{2k-1} \quad (\text{A5a})$$

$$= c_{2k}^\dagger c_{2k-1} \quad (\text{A5b})$$

where we have used that $\tilde{\phi}_{2k} \tilde{\phi}_{2k+1} = 1 - 2c_{2k-1}^\dagger c_{2k-1}$ so that JW strings between sequential fermionic operators cancel out.

All of this means that

$$|\Psi_R\rangle \xrightarrow{\text{JW}} \left[\prod_{k=1}^{M/2} (1 - c_{2k}^\dagger c_{2k-1}) \right] |1010\dots\rangle \quad (\text{A6a})$$

$$= \left[\prod_{k=1}^{M/2} e^{-c_{2k}^\dagger c_{2k-1}} \right] |1010\dots\rangle \quad (\text{A6b})$$

$$= e^{-\sum_{k=1}^{M/2} c_{2k}^\dagger c_{2k-1}} |1010\dots\rangle, \quad (\text{A6c})$$

which is the Thouless representation of an HF state. Thus, HF is already energetically exact in the $G \rightarrow -\infty$ limit of the JW-transformed pairing Hamiltonian, and as HF is a special case of PHFB, this means PHFB is also energetically exact.

Appendix B: The 8-Site Bravyi-Kitaev and Sierpinski Transformations

For the JW and Π transformations, it is straightforward to write down both the mapping from fermions to spins and the inverse mapping from spins back to fermions. For the BK and Sierpinski mappings, this is less easy. Accordingly, we note the 8-site mappings we have used here. More specifically, we record the mappings from the Pauli operators σ^x and σ^z to the Majoranas; we extract σ^y from

$$\sigma_p^z \sigma_p^x = i \sigma_p^y. \quad (\text{B1})$$

For brevity we define the Majorana products

$$A_p = i \gamma_{1,p} \gamma_{2,p} = 1 - 2 c_p^\dagger c_p, \quad (\text{B2a})$$

$$B_p = i \gamma_{2,p} \gamma_{1,p+1}. \quad (\text{B2b})$$

These objects are Hermitian, mutually commuting, and satisfy $A_p^2 = B_p^2 = 1$. They also commute with individual Majorana operators, except that they anticommute with their constituents, i.e., A_p anticommutes with $\gamma_{1,p}$ and $\gamma_{2,p}$ while B_p anticommutes with $\gamma_{1,p+1}$ and $\gamma_{2,p}$.

The 8-site BK spin-to-fermion mapping is

$$\sigma_{1, \text{BK}}^x \mapsto B_1 \quad \sigma_{1, \text{BK}}^z \mapsto A_1, \quad (\text{B3a})$$

$$\sigma_{2, \text{BK}}^x \mapsto B_2 B_3 \quad \sigma_{2, \text{BK}}^z \mapsto A_1 A_2, \quad (\text{B3b})$$

$$\sigma_{3, \text{BK}}^x \mapsto B_3 \quad \sigma_{3, \text{BK}}^z \mapsto A_3, \quad (\text{B3c})$$

$$\sigma_{4, \text{BK}}^x \mapsto B_4 B_5 B_6 B_7 \quad \sigma_{4, \text{BK}}^z \mapsto A_1 A_2 A_3 A_4, \quad (\text{B3d})$$

$$\sigma_{5, \text{BK}}^x \mapsto B_5 \quad \sigma_{5, \text{BK}}^z \mapsto A_5, \quad (\text{B3e})$$

$$\sigma_{6, \text{BK}}^x \mapsto B_6 B_7 \quad \sigma_{6, \text{BK}}^z \mapsto A_5 A_6, \quad (\text{B3f})$$

$$\sigma_{7, \text{BK}}^x \mapsto B_7 \quad \sigma_{7, \text{BK}}^z \mapsto A_7, \quad (\text{B3g})$$

$$\sigma_{8, \text{BK}}^x \mapsto -i \Pi \gamma_{2,8} \quad \sigma_{8, \text{BK}}^z \mapsto \Pi, \quad (\text{B3h})$$

while the 8-site Sierpinski spin-to-fermion mapping is in-

stead

$$\sigma_1^x \mapsto_S B_1 \quad \sigma_1^z \mapsto_S A_1, \quad (\text{B4a})$$

$$\sigma_2^x \mapsto_S B_2 B_3 B_4 \quad \sigma_2^z \mapsto_S A_1 A_2 A_3, \quad (\text{B4b})$$

$$\sigma_3^x \mapsto_S B_2 \quad \sigma_3^z \mapsto_S A_3, \quad (\text{B4c})$$

$$\sigma_4^x \mapsto_S B_4 \quad \sigma_4^z \mapsto_S A_4, \quad (\text{B4d})$$

$$\sigma_5^x \mapsto_S B_1 B_2 B_3 B_4 \gamma_{1,1} \quad \sigma_5^z \mapsto_S \Pi A_7 A_8, \quad (\text{B4e})$$

$$\sigma_6^x \mapsto_S B_5 \quad \sigma_6^z \mapsto_S A_6, \quad (\text{B4f})$$

$$\sigma_7^x \mapsto_S B_7 \quad \sigma_7^z \mapsto_S A_7, \quad (\text{B4g})$$

$$\sigma_8^x \mapsto_S i \Pi \gamma_{2,8} \quad \sigma_8^z \mapsto_S A_7 A_8. \quad (\text{B4h})$$

Overall signs are arbitrary, but factors of i are not. Ultimately, this is because we can multiply any two Paulis by -1 without changing the $\mathfrak{su}(2)$ commutation rules.

Recall that Π is the number parity operator (c.f. Eqn. (18b)), given in this notation as

$$\Pi = \prod_p A_p. \quad (\text{B5})$$

-
- [1] C. D. Batista and G. Ortiz, in *Condensed Matter Theories*, Vol. 16, edited by S. Hernandez and W. J. Clark (Nova Science Publishers, Inc, Huntington, New York, 2001) pp. 1–15.
- [2] H. Nishimori and G. Ortiz, *Elements of Phase Transitions and Critical Phenomena* (Oxford University Press, Oxford, 2011) p. 220.
- [3] P. Jordan and E. Wigner, *Zeitschrift für Physik* **47**, 631 (1928).
- [4] L. L. Gonçalves, L. P. S. Coutinho, and J. P. de Lima, *Physica A* **345**, 71 (2005).
- [5] T. Verkholyak, A. Honecker, and W. Brenig, *Eur. Phys. J. B* **49**, 283 (2006).
- [6] A. Kitaev and C. Laumann, “Topological phases and quantum computation,” Lectures given by Alexei Kitaev at the 2008 Les Houches summer school “Exact methods in low-dimensional physics and quantum computing.” (2008).
- [7] T. Verkholyak, J. Strečka, M. Jaščur, and J. Richter, *Acta Phys. Pol. A* **118**, 978 (2010).
- [8] C.-E. Bardyn and A. Imamoglu, *Phys. Rev. Lett.* **109**, 253606 (2012).
- [9] A. A. Zvyagin, *Phs. Rev. Lett.* **110**, 217207 (2013).
- [10] M. Greiter, V. Schnells, and R. Thomale, *Ann. Phys.* **351**, 1026 (2014).
- [11] F. Gebhard, K. Bauerbach, and Ö. Legeza, *Phys. Rev. B* **106**, 205133 (2022).
- [12] T. M. Henderson, G. P. Chen, and G. E. Scuseria, *J. Chem. Phys.* **157**, 194114 (2022).
- [13] T. M. Henderson, F. Gao, and G. E. Scuseria, *Mol. Phys.* **122**, e2254857 (2024).
- [14] S. B. Bravyi and A. Y. Kitaev, *Ann. Phys.* **298**, 210 (2002).
- [15] Y. Cao, J. Romero, J. P. Olson, M. Degroote, P. D. Johnson, M. Kieferová, I. D. Kivlichan, T. Menke, B. Peropadre, N. P. D. Sawaya, S. Sim, L. Veis, and A. Aspuru-Guzik, *Chem. Rev.* **119**, 10856 (2019).
- [16] B. Bauer, S. Bravyi, M. Motta, and G. K. Chan, *Chem. Rev.* **120**, 12685 (2020).
- [17] S. McArdle, S. Endo, A. Aspuru-Guzik, S. C. Benjamin, and X. Yuan, *Rev. Mod. Phys.* **92**, 015003 (2020).
- [18] F. Verstraete and J. I. Cirac, *J. Stat. Mech.* **2005**, P09012 (2005).
- [19] J. T. Seeley, M. J. Richard, and P. J. Love, *J. Chem. Phys.* **137**, 224109 (2012).
- [20] V. Havlíček, M. Troyer, and J. D. Whitfield, *Phys. Rev. A* **95**, 032332 (2017).
- [21] S. Bravyi, J. M. Gambetta, A. Mezzacapo, and K. Temme, “Tapering off qubits to simulate fermionic hamiltonians,” (2017), arXiv:1701.08213 [quant-ph].
- [22] K. Setia, S. Bravyi, A. Mezzacapo, and J. D. Whitfield, *Phys. Rev. Res.* **1**, 033033 (2019).
- [23] Z. Jiang, A. Kalev, W. Mruczkiewicz, and H. Neven, *Quantum* **4**, 276 (2020).
- [24] D. Picozzi and J. Tennyson, *Quantum Sci. Technol.* **8**, 035026 (2023).
- [25] Y. Liu, S. Che, J. Zhou, Y. Shi, and G. Li, in *ASPLOS 2024* (2024).
- [26] B. Harrison, D. Nelson, D. Adamiak, and J. Whitfield, “Reducing the qubit requirement of Jordan-Wigner encodings of n -mode, k -fermion systems from n to $\lceil \log_2 \binom{N}{K} \rceil$,” (2023), arXiv:2211.04501 [quant-ph].

- [27] O. O'Brien and S. Strelchuk, *Phys. Rev. B* **109**, 115149 (2024).
- [28] B. Harrison, M. Chiew, J. Necaïse, A. Projansky, S. Strelchuk, and J. D. Whitfield, "A Sierpinski triangle fermion-to-qubit transform," (2024), arXiv:2409.04348 [quant-ph].
- [29] H. Fukutome, M. Yamamura, and S. Nishiyama, *Prog. Theor. Phys.* **57**, 1554 (1977).
- [30] H. Fukutome, *Prog. Theor. Phys.* **58**, 1692 (1977).
- [31] J. E. Moussa, "Generalized unitary Bogoliubov transformation that breaks fermion number parity," (2012), arXiv:1208.1086 [cond-mat.str-el].
- [32] T. M. Henderson, S. Ghassemi Tabrizi, G. P. Chen, and G. E. Scuseria, *J. Chem. Phys.* **160**, 064103 (2024).
- [33] M. Chiew and S. Strelchuk, *Quantum* **7**, 1145 (2023).
- [34] Y. R. Wang, *Phys. Rev. B* **43**, 3786 (1991).
- [35] A. Tranter, S. Sofia, J. Seeley, M. Kaicher, J. McClean, R. Babbush, P. V. Coveney, F. Mintert, F. Wilhelm, and P. J. Love, *International Journal of Quantum Chemistry* **115**, 1431 (2015), <https://onlinelibrary.wiley.com/doi/pdf/10.1002/qua.24969>.
- [36] D. J. Thouless, *Nucl. Phys.* **21**, 225 (1960).
- [37] V. Bach, E. H. Lieb, and J. P. Solovej, *J. Stat. Phys.* **76**, 3 (1994).
- [38] J. H. P. Colpa, *J. Phys. A: Math. Gen.* **12**, 49 (1979).
- [39] S. Nishiyama and J. da Providência, *Internat. J. Geom. Meth. in Mod. Phys.* **16**, 1950184 (2019).
- [40] R. Balian and E. Brezin, *Il Nuovo Cimento B* **64**, 37 (1969).
- [41] G. P. Chen and G. E. Scuseria, *J. Chem. Phys.* **158**, 231102 (2023).
- [42] U. Schollwöck, J. Richter, D. J. J. Farnell, and R. F. Bishop, eds., *Quantum Magnetism* (Springer, Berlin, Heidelberg, 2004).
- [43] P. Carretta, R. Melzi, N. Papinutto, and P. Millet, *Phys. Rev. Lett.* **88**, 047601 (2002).
- [44] A. Bombardi, J. Rodriguez-Carvajal, S. Di Matteo, F. de Bergevin, L. Paolasini, P. Carretta, P. Millet, and R. Caciuffo, *Phys. Rev. Lett.* **93**, 027202 (2004).
- [45] M. Rams, A. Jochim, M. Böhme, T. Lohmiller, M. Ceglarska, M. M. Rams, A. Schnegg, W. Plass, and C. Näther, *Chem. Eur. J* **26**, 2837 (2020).
- [46] J. Bardeen, L. N. Cooper, and J. R. Schrieffer, *Phys. Rev.* **108**, 1175 (1957).
- [47] G. Sierra, J. Dukelsky, G. G. Dussel, J. von Delft, and F. Braun, *Phys. Rev. B* **61**, R11890 (2000).
- [48] R. Darradi, O. Derzhko, R. Zinke, J. Schulenburg, S. E. Krüger, and J. Richter, *Phys. Rev. B* **78**, 214415 (2008).
- [49] S.-S. Gong, W. Zhu, D. N. Sheng, O. I. Motrunich, and M. P. A. Fisher, *Phys. Rev. Lett.* **113**, 027201 (2014).
- [50] J. Richter, R. Zinke, and D. J. J. Farnell, *Eur. Phys. J. B* **88**, 2 (2015).
- [51] C. Majumdar and D. K. Ghosh, *J. Math. Phys.* **10**, 1388 (1969).
- [52] G. E. Massaccesi, A. Rubio-García, P. Capuzzi, E. Ríos, O. B. Oña, J. Dukelsky, L. Lain, A. Torre, and D. R. Alcoba, *J. Stat. Mech.* **2021**, 013110 (2021).
- [53] Z. Liu, F. Gao, G. P. Chen, T. M. Henderson, J. Dukelsky, and G. E. Scuseria, *Phys. Rev. B* **108**, 085136 (2023).
- [54] D. J. J. Farnell and R. F. Bishop, "The coupled cluster method applied to quantum magnetism," in *Quantum Magnetism*, edited by U. Schollwöck, J. Richter, D. J. J. Farnell, and R. F. Bishop (Springer, Berlin, Heidelberg, 2004) pp. 307–348.
- [55] R. W. Richardson, *Phys. Lett.* **3**, 277 (1963).
- [56] R. W. Richardson and N. Sherman, *Nucl. Phys.* **52**, 221 (1964).
- [57] R. W. Richardson, *J. Math. Phys.* **6**, 1034 (1965).
- [58] E. A. Yuzbashyan, A. A. Baytin, and B. L. Altshuler, *Phys. Rev. B* **68**, 214509 (2003).
- [59] A. Faribault, P. Calabrese, and J.-S. Caux, *Phys. Rev. B* **81**, 174507 (2010).
- [60] P. A. Johnson, "Richardson-Gaudin States," (2023), arXiv:2312.08804 [physics.chem-ph].
- [61] J. A. Sheikh and P. Ring, *Nucl. Phys. A* **665**, 71 (2000).
- [62] K. Schmid, *Prog. Part. Nucl. Phys.* **52**, 565 (2004).
- [63] G. E. Scuseria, C. A. Jiménez-Hoyos, T. M. Henderson, K. Samanta, and J. K. Ellis, *J. Chem. Phys.* **135**, 124108 (2011).

Supplementary Material for Fermionic Mean-Field Theory as a Tool for Studying Spin Hamiltonians

PROOF THAT A SPIN MEAN-FIELD WAVE FUNCTION MAPS TO A FERMIONIC MEAN-FIELD WAVE FUNCTION

In this note we prove that a spin mean-field wave function of the form $|\text{BCS}\rangle = \exp(\sum_p t_p S_p^+) |\Downarrow\rangle$ maps, under Jordan–Wigner transformation, to a special case of the Hartree–Fock–Bogoliubov–Fukutome transformation. Specifically, we show that

$$e^{\sum_p t_p S_p^+} |\Downarrow\rangle \xrightarrow{\text{JW}} \left(1 + \sum t_p c_p^\dagger\right) e^{\sum_{p<q} t_p t_q c_p^\dagger c_q^\dagger} |-\rangle. \quad (\text{S1})$$

We begin by expanding the spin mean-field state in different S_z sectors. This gives us

$$e^{\sum_p t_p S_p^+} |\Downarrow\rangle = \left(1 + \sum_p t_p S_p^+ + \frac{1}{2} \sum_{pq} t_p t_q S_p^+ S_q^+ + \frac{1}{3!} \sum_{pqr} t_p t_q t_r S_p^+ S_q^+ S_r^+ + \dots\right) |\Downarrow\rangle. \quad (\text{S2})$$

Because the individual S_p^+ commute and are nilpotent ($S_p^+ S_p^+ = 0$) we can write equivalently

$$e^{\sum_p t_p S_p^+} |\Downarrow\rangle = \left(1 + \sum_p t_p S_p^+ + \frac{1}{2} \sum_{p \neq q} t_p t_q S_p^+ S_q^+ + \frac{1}{3!} \sum_{p \neq q \neq r} t_p t_q t_r S_p^+ S_q^+ S_r^+ + \dots\right) |\Downarrow\rangle \quad (\text{S3a})$$

$$= \left(1 + \sum_p t_p S_p^+ + \sum_{p<q} t_p t_q S_p^+ S_q^+ + \sum_{p<q<r} t_p t_q t_r S_p^+ S_q^+ S_r^+ + \dots\right) |\Downarrow\rangle. \quad (\text{S3b})$$

Now we Jordan–Wigner-transform this wave function. The spin vacuum $|\Downarrow\rangle$ transforms into the fermionic physical vacuum $|-\rangle$, while

$$S_p^+ \xrightarrow{\text{JW}} c_p^\dagger \tilde{\phi}_p, \quad (\text{S4a})$$

$$\tilde{\phi}_p = \prod_{k<p} (1 - 2n_k), \quad (\text{S4b})$$

$$n_k = c_k^\dagger c_k. \quad (\text{S4c})$$

This means that

$$|\text{BCS}\rangle \xrightarrow{\text{JW}} \left(1 + \sum_p t_p c_p^\dagger \tilde{\phi}_p + \sum_{p<q} t_p t_q c_p^\dagger \tilde{\phi}_p c_q^\dagger \tilde{\phi}_q + \sum_{p<q<r} t_p t_q t_r c_p^\dagger \tilde{\phi}_p c_q^\dagger \tilde{\phi}_q c_r^\dagger \tilde{\phi}_r + \dots\right) |-\rangle. \quad (\text{S5})$$

Because $\tilde{\phi}_p$ commutes with c_q^\dagger for $q \geq p$ and we have written the operators in ascending order, the JW strings $\tilde{\phi}_p$ commute to the right where they meet the physical vacuum $|-\rangle$, for which we can use

$$\tilde{\phi}_p |-\rangle = |-\rangle. \quad (\text{S6})$$

Thus, we have

$$|\text{BCS}\rangle \xrightarrow{\text{JW}} \left(1 + \sum_p t_p c_p^\dagger + \sum_{p<q} t_p t_q c_p^\dagger c_q^\dagger + \sum_{p<q<r} t_p t_q t_r c_p^\dagger c_q^\dagger c_r^\dagger + \dots\right) |-\rangle. \quad (\text{S7})$$

We must prove that

$$\left(1 + \sum_p t_p c_p^\dagger + \sum_{p<q} t_p t_q c_p^\dagger c_q^\dagger + \sum_{p<q<r} t_p t_q t_r c_p^\dagger c_q^\dagger c_r^\dagger + \dots\right) |-\rangle = \left(1 + \sum t_p c_p^\dagger\right) e^{\sum_{p<q} t_p t_q c_p^\dagger c_q^\dagger} |-\rangle. \quad (\text{S8})$$

A Useful Identity

Let us begin with a useful identity:

$$\sum_{p_1 < \dots < p_m} \sum_{p_{m+1} > p_k} t_{p_1} \dots t_{p_{m+1}} c_{p_1}^\dagger \dots c_{p_{m+1}}^\dagger = \begin{cases} \sum_{p_1 < \dots < p_{m+1}} t_{p_1} \dots t_{p_{m+1}} c_{p_1}^\dagger \dots c_{p_{m+1}}^\dagger & m - k \text{ even,} \\ 0 & m - k \text{ odd,} \end{cases} \quad (\text{S9})$$

with $p_k \in \{0, p_1, \dots, p_m\}$.

To see this, we begin by examining the simpler case where the second summation is restricted by an upper limit of p_{k+1} , which enforces an ordering between the indices in the two summations:

$$\sum_{p_1 < \dots < p_m} \sum_{p_{m+1} > p_k}^{p_{k+1}} t_{p_1} \dots t_{p_{m+1}} c_{p_1}^\dagger \dots c_{p_{m+1}}^\dagger = (-1)^{m-k} \sum_{p_1 < \dots < p_m} \sum_{p_{m+1} > p_k}^{p_{k+1}} t_{p_1} \dots t_{p_{m+1}} c_{p_1}^\dagger \dots c_{p_k}^\dagger c_{p_{m+1}}^\dagger c_{p_{k+1}}^\dagger \dots c_{p_m}^\dagger \quad (\text{S10a})$$

$$= (-1)^{m-k} \sum_{p_1 < \dots < p_{m+1}} t_{p_1} \dots t_{p_{m+1}} c_{p_1}^\dagger \dots c_{p_{m+1}}^\dagger, \quad (\text{S10b})$$

where we used the fact that fermionic creation operators are nilpotent to eliminate the $p_{m+1} = p_{k+1}$ term and strictly order the indices. In the special case that $k = m$, the upper limit of the summation over p_{m+1} is M , where M is the number of levels; if $p_k = 0$ then the lower limit of the summation over p_{m+1} is 1. In the first line, we have anticommutated $c_{p_{m+1}}^\dagger$ to the left $m - k$ times to sort the creation operators in ascending order of their indices. This gives us a plus or minus sign, depending on whether $m - k$ is an even (plus sign) or an odd (minus sign) number. In the second line, we have relabeled the indices, renaming $p_{m+1} \rightarrow p_{k+1}$, $p_{k+1} \rightarrow p_{k+2}$, and so on. The relabeling naturally has no effect on the coefficient since it is completely factorized.

Using Eqn. (S10), we can prove Eqn. (S9).

Let us start with the expression on the left-hand side of Eqn. (S9), in which the second summation runs over $p_{m+1} \in (p_k, M]$. We divide this range into pieces: $(p_k, p_{k+1}]$, $(p_{k+1}, p_{k+2}]$, and so on, ending with $(p_m, M]$. There are two cases to consider. If $m - k$ is even, i.e., $k = m - 2j$, there are $2j + 1$ such pieces. Applying the identity of Eqn. (S10) to each, we see that all these pieces are identical, save that $j + 1$ of them appear with a plus sign and j of them appear with a minus sign. All but one of these pieces thus cancel each other, and we are left with

$$\sum_{p_1 < \dots < p_m} \sum_{p_{m+1} > p_{m-2j}} t_{p_1} \dots t_{p_{m+1}} c_{p_1}^\dagger \dots c_{p_{m+1}}^\dagger = \sum_{p_1 < \dots < p_{m+1}} t_{p_1} \dots t_{p_{m+1}} c_{p_1}^\dagger \dots c_{p_{m+1}}^\dagger. \quad (\text{S11})$$

When $m - k$ is odd ($k = m - 2j - 1$), we instead divide the range $(p_k, M]$ into an even number of pieces. These pieces are identical, save that half of them appear with a plus sign and half with a minus sign. The entire summation thus adds to zero:

$$\sum_{p_1 < \dots < p_m} \sum_{p_{m+1} > p_{m-2j-1}} t_{p_1} \dots t_{p_{m+1}} c_{p_1}^\dagger \dots c_{p_{m+1}}^\dagger = 0. \quad (\text{S12})$$

Equations (S11) and (S12) together prove our target, Eqn. (S9).

Terms in the Left-Hand-Side of Eqn. (S8) With an Even Number of Fermionic Operators

Our task here is to prove that

$$\frac{1}{n!} \left(\sum_{p < q} t_p t_q c_p^\dagger c_q^\dagger \right)^n = \sum_{p_1 < \dots < p_{2n}} t_{p_1} \dots t_{p_{2n}} c_{p_1}^\dagger \dots c_{p_{2n}}^\dagger. \quad (\text{S13})$$

We will do so inductively.

For $n = 1$ this is trivially true. We must show that Eqn. (S13) is true for $n + 1$ if it is true for n . That is, we must show that

$$\frac{1}{(n+1)!} \left(\sum_{p < q} t_p t_q c_p^\dagger c_q^\dagger \right)^{n+1} = \sum_{p_1 < \dots < p_{2n+2}} t_{p_1} \dots t_{p_{2n+2}} c_{p_1}^\dagger \dots c_{p_{2n+2}}^\dagger. \quad (\text{S14})$$

Now, assuming that Eqn. (S13) is true for n , we have

$$\frac{1}{(n+1)!} \left(\sum_{p < q} t_p t_q c_p^\dagger c_q^\dagger \right)^{n+1} = \frac{1}{n+1} \sum_{p_1 < \dots < p_{2n}} t_{p_1} \dots t_{p_{2n}} c_{p_1}^\dagger \dots c_{p_{2n}}^\dagger \sum_{p_{2n+1} < p_{2n+2}} t_{p_{2n+1}} t_{p_{2n+2}} c_{p_{2n+1}}^\dagger c_{p_{2n+2}}^\dagger. \quad (\text{S15})$$

Divide the summation over p_{2n+1} into the $2n+1$ distinct ranges: $p_{2n+1} < p_1$, and $p_1 < p_{2n+1} < p_2$, and so on. After anticommuting $c_{p_{2n+1}}^\dagger$ into the appropriate position so that the operators $c_{p_1}^\dagger \dots c_{p_{2n+1}}^\dagger$ appear in ascending order, we have

$$\begin{aligned} \frac{1}{(n+1)!} \left(\sum_{p < q} t_p t_q c_p^\dagger c_q^\dagger \right)^{n+1} &= \frac{1}{n+1} \sum_{p_1 < \dots < p_{2n+1}} t_{p_1} \dots t_{p_{2n+2}} c_{p_1}^\dagger \dots c_{p_{2n+1}}^\dagger \sum_{p_{2n+2} > p_{2n+1}} c_{p_{2n+2}}^\dagger \\ &- \frac{1}{n+1} \sum_{p_1 < \dots < p_{2n+1} < p_{2n}} t_{p_1} \dots t_{p_{2n+2}} c_{p_1}^\dagger \dots c_{p_{2n+1}}^\dagger c_{p_{2n}}^\dagger \sum_{p_{2n+2} > p_{2n+1}} c_{p_{2n+2}}^\dagger \\ &+ \dots \\ &+ \frac{1}{n+1} \sum_{p_{2n+1} < p_1 < \dots < p_{2n}} t_{p_1} \dots t_{p_{2n+2}} c_{p_{2n+1}}^\dagger c_{p_1}^\dagger \dots c_{p_{2n}}^\dagger \sum_{p_{2n+2} > p_{2n+1}} c_{p_{2n+2}}^\dagger. \end{aligned} \quad (\text{S16})$$

It will prove helpful to relabel indices p_1 through p_{2n+1} at this point:

$$\begin{aligned} \frac{1}{(n+1)!} \left(\sum_{p < q} t_p t_q c_p^\dagger c_q^\dagger \right)^{n+1} &= \frac{1}{n+1} \sum_{p_1 < \dots < p_{2n+1}} t_{p_1} \dots t_{p_{2n+2}} c_{p_1}^\dagger \dots c_{p_{2n+1}}^\dagger \sum_{p_{2n+2} > p_{2n+1}} c_{p_{2n+2}}^\dagger \\ &- \frac{1}{n+1} \sum_{p_1 < \dots < p_{2n+1}} t_{p_1} \dots t_{p_{2n+2}} c_{p_1}^\dagger \dots c_{p_{2n+1}}^\dagger \sum_{p_{2n+2} > p_{2n}} c_{p_{2n+2}}^\dagger \\ &+ \dots \\ &+ \frac{1}{n+1} \sum_{p_1 < \dots < p_{2n+1}} t_{p_1} \dots t_{p_{2n+2}} c_{p_1}^\dagger \dots c_{p_{2n+1}}^\dagger \sum_{p_{2n+2} > p_1} c_{p_{2n+2}}^\dagger. \end{aligned} \quad (\text{S17})$$

Now we apply the identity of Eqn. (S9) to each line sequentially. Doing so reveals that the odd lines (those with plus signs) are all identical, and the even lines (those with minus signs) all vanish. For example, the first line on the right-hand-side of Eqn. (S17) has $m = 2n + 1$ and $k = m$ so that $m - k = 0$; the second line has $m - k = 1$, and so on. We have $n + 1$ odd lines, and this factor of $n + 1$ exactly cancels the $\frac{1}{n+1}$ on each line, completing the proof.

Let us give an example for concreteness. We will consider the case $n = 2$, so we have

$$\mathcal{O} = \frac{1}{2} \sum_{p_1 < p_2} \sum_{p_3 < p_4} t_{p_1} \dots t_{p_4} c_{p_1}^\dagger c_{p_2}^\dagger c_{p_3}^\dagger c_{p_4}^\dagger. \quad (\text{S18})$$

We break the summation over p_3 into 3 distinct ranges, resulting in

$$\begin{aligned} \mathcal{O} &= \frac{1}{2} \sum_{p_1 < p_2 < p_3} \sum_{p_4 > p_3} t_{p_1} \dots t_{p_4} c_{p_1}^\dagger c_{p_2}^\dagger c_{p_3}^\dagger c_{p_4}^\dagger \\ &+ \frac{1}{2} \sum_{p_1 < p_3 < p_2} \sum_{p_4 > p_3} t_{p_1} \dots t_{p_4} c_{p_1}^\dagger c_{p_2}^\dagger c_{p_3}^\dagger c_{p_4}^\dagger \\ &+ \frac{1}{2} \sum_{p_3 < p_1 < p_2} \sum_{p_4 > p_3} t_{p_1} \dots t_{p_4} c_{p_1}^\dagger c_{p_2}^\dagger c_{p_3}^\dagger c_{p_4}^\dagger. \end{aligned} \quad (\text{S19})$$

Anticommute $c_{p_3}^\dagger$ into the correct position:

$$\begin{aligned} \mathcal{O} &= \frac{1}{2} \sum_{p_1 < p_2 < p_3} \sum_{p_4 > p_3} t_{p_1} \dots t_{p_4} c_{p_1}^\dagger c_{p_2}^\dagger c_{p_3}^\dagger c_{p_4}^\dagger \\ &\quad - \frac{1}{2} \sum_{p_1 < p_3 < p_2} \sum_{p_4 > p_3} t_{p_1} \dots t_{p_4} c_{p_1}^\dagger c_{p_3}^\dagger c_{p_2}^\dagger c_{p_4}^\dagger \\ &\quad + \frac{1}{2} \sum_{p_3 < p_1 < p_2} \sum_{p_4 > p_3} t_{p_1} \dots t_{p_4} c_{p_3}^\dagger c_{p_1}^\dagger c_{p_2}^\dagger c_{p_4}^\dagger. \end{aligned} \quad (\text{S20})$$

Relabel for convenience:

$$\begin{aligned} \mathcal{O} &= \frac{1}{2} \sum_{p_1 < p_2 < p_3} \sum_{p_4 > p_3} t_{p_1} \dots t_{p_4} c_{p_1}^\dagger c_{p_2}^\dagger c_{p_3}^\dagger c_{p_4}^\dagger \\ &\quad - \frac{1}{2} \sum_{p_1 < p_2 < p_3} \sum_{p_4 > p_2} t_{p_1} \dots t_{p_4} c_{p_1}^\dagger c_{p_2}^\dagger c_{p_3}^\dagger c_{p_4}^\dagger \\ &\quad + \frac{1}{2} \sum_{p_1 < p_2 < p_3} \sum_{p_4 > p_1} t_{p_1} \dots t_{p_4} c_{p_1}^\dagger c_{p_2}^\dagger c_{p_3}^\dagger c_{p_4}^\dagger. \end{aligned} \quad (\text{S21})$$

Now break the summations over p_4 into separate ranges:

$$\begin{aligned} \mathcal{O} &= \left(\frac{1}{2} \sum_{p_1 < p_2 < p_3} \sum_{p_4 > p_3} t_{p_1} \dots t_{p_4} c_{p_1}^\dagger c_{p_2}^\dagger c_{p_3}^\dagger c_{p_4}^\dagger \right) \\ &\quad - \left(\frac{1}{2} \sum_{p_1 < p_2 < p_3} \sum_{p_4 > p_2} t_{p_1} \dots t_{p_4} c_{p_1}^\dagger c_{p_2}^\dagger c_{p_3}^\dagger c_{p_4}^\dagger + \frac{1}{2} \sum_{p_1 < p_2 < p_3} \sum_{p_4 > p_3} t_{p_1} \dots t_{p_4} c_{p_1}^\dagger c_{p_2}^\dagger c_{p_3}^\dagger c_{p_4}^\dagger \right) \\ &\quad + \left(\frac{1}{2} \sum_{p_1 < p_2 < p_3} \sum_{p_4 > p_1} t_{p_1} \dots t_{p_4} c_{p_1}^\dagger c_{p_2}^\dagger c_{p_3}^\dagger c_{p_4}^\dagger + \frac{1}{2} \sum_{p_1 < p_2 < p_3} \sum_{p_4 > p_2} t_{p_1} \dots t_{p_4} c_{p_1}^\dagger c_{p_2}^\dagger c_{p_3}^\dagger c_{p_4}^\dagger \right) \\ &\quad + \left. \sum_{p_1 < p_2 < p_3} \sum_{p_4 > p_3} t_{p_1} \dots t_{p_4} c_{p_1}^\dagger c_{p_2}^\dagger c_{p_3}^\dagger c_{p_4}^\dagger \right). \end{aligned} \quad (\text{S22})$$

Note that each set of terms enclosed in parentheses corresponds to a single line of Eqn. (S21).

Anticommute $c_{p_4}^\dagger$ into the appropriate positions:

$$\begin{aligned} \mathcal{O} &= \left(\frac{1}{2} \sum_{p_1 < p_2 < p_3} \sum_{p_4 > p_3} t_{p_1} \dots t_{p_4} c_{p_1}^\dagger c_{p_2}^\dagger c_{p_3}^\dagger c_{p_4}^\dagger \right) \\ &\quad + \left(\frac{1}{2} \sum_{p_1 < p_2 < p_3} \sum_{p_4 > p_2} t_{p_1} \dots t_{p_4} c_{p_1}^\dagger c_{p_2}^\dagger c_{p_4}^\dagger c_{p_3}^\dagger - \frac{1}{2} \sum_{p_1 < p_2 < p_3} \sum_{p_4 > p_3} t_{p_1} \dots t_{p_4} c_{p_1}^\dagger c_{p_2}^\dagger c_{p_3}^\dagger c_{p_4}^\dagger \right) \\ &\quad + \left(\frac{1}{2} \sum_{p_1 < p_2 < p_3} \sum_{p_4 > p_1} t_{p_1} \dots t_{p_4} c_{p_1}^\dagger c_{p_4}^\dagger c_{p_2}^\dagger c_{p_3}^\dagger - \frac{1}{2} \sum_{p_1 < p_2 < p_3} \sum_{p_4 > p_2} t_{p_1} \dots t_{p_4} c_{p_1}^\dagger c_{p_2}^\dagger c_{p_4}^\dagger c_{p_3}^\dagger \right) \\ &\quad + \left. \frac{1}{2} \sum_{p_1 < p_2 < p_3} \sum_{p_4 > p_3} t_{p_1} \dots t_{p_4} c_{p_1}^\dagger c_{p_2}^\dagger c_{p_3}^\dagger c_{p_4}^\dagger \right). \end{aligned} \quad (\text{S23})$$

After relabeling, we see that the first and third set of terms are identical and the second set of terms vanishes, so we have

$$\mathcal{O} = \sum_{p_1 < p_2 < p_3 < p_4} t_{p_1} \dots t_{p_4} c_{p_1}^\dagger c_{p_2}^\dagger c_{p_3}^\dagger c_{p_4}^\dagger. \quad (\text{S24})$$

Terms in the Left-Hand-Side of Eqn. (S8) With an Odd Number of Fermionic Operators

It remains to prove that

$$\left(\sum_{p_1 < \dots < p_{2n+1}} t_{p_1} \dots t_{p_{2n+1}} c_{p_1}^\dagger \dots c_{p_{2n+1}}^\dagger \right) \sum_{p_1 < \dots < p_{2n}} t_{p_1} \dots t_{p_{2n}} c_{p_1}^\dagger \dots c_{p_{2n}}^\dagger = \sum_{p_1 < p_2 < \dots < p_{2n+1}} t_{p_1} \dots t_{p_{2n+1}} c_{p_1}^\dagger \dots c_{p_{2n+1}}^\dagger. \quad (\text{S25})$$

After anticommuting $c_{p_{2n+1}}^\dagger$ all the way to the right (using the fact that if any two indices are equal the term vanishes, and otherwise we have anticommutated through an even number of operators), this is a straightforward application of Eqn. S9 where $m = 2n$ and $k = 0$.

The Final Result

We have seen that

$$\sum_{p_1 < \dots < p_{2n}} t_{p_1} \dots t_{p_{2n}} c_{p_1}^\dagger \dots c_{p_{2n}}^\dagger = \frac{1}{n!} \left(\sum_{p < q} t_p t_q c_p^\dagger c_q^\dagger \right)^n, \quad (\text{S26a})$$

$$\sum_{p_1 < \dots < p_{2n+1}} t_{p_1} \dots t_{p_{2n+1}} c_{p_1}^\dagger \dots c_{p_{2n+1}}^\dagger = \left(\sum_{p_{2n+1}} t_{p_{2n+1}} c_{p_{2n+1}}^\dagger \right) \sum_{p_1 < p_2 < \dots < p_{2n}} t_{p_1} \dots t_{p_{2n}} c_{p_1}^\dagger \dots c_{p_{2n}}^\dagger. \quad (\text{S26b})$$

From the first result, we have that

$$e^{\sum_{p < q} t_p t_q c_p^\dagger c_q^\dagger} = 1 + \sum_{p < q} t_p t_q c_p^\dagger c_q^\dagger + \sum_{p < q < r < s} t_p t_q t_r t_s c_p^\dagger c_q^\dagger c_r^\dagger c_s^\dagger + \dots \quad (\text{S27})$$

The two lines together mean that

$$\sum_p t_p c_p^\dagger e^{\sum_{p < q} t_p t_q c_p^\dagger c_q^\dagger} = \sum_p t_p c_p^\dagger + \sum_{p < q < r} t_p t_q t_r c_p^\dagger c_q^\dagger c_r^\dagger + \sum_{p < q < r < s < t} t_p t_q t_r t_s t_t c_p^\dagger c_q^\dagger c_r^\dagger c_s^\dagger c_t^\dagger + \dots \quad (\text{S28})$$

Overall, we therefore have

$$\left(1 + \sum_p t_p c_p^\dagger \right) e^{\sum_{p < q} t_p t_q c_p^\dagger c_q^\dagger} |-\rangle = \left(1 + \sum_p t_p c_p^\dagger + \sum_{p < q} t_p t_q c_p^\dagger c_q^\dagger + \sum_{p < q < r} t_p t_q t_r c_p^\dagger c_q^\dagger c_r^\dagger + \dots \right) |-\rangle. \quad (\text{S29})$$

This is what we wished, ultimately, to prove: the right-hand-side is the JW-transformation of the spin mean-field state, and the left-hand-side is a special case of an HFBF fermionic mean-field. This means that any $\mathfrak{su}(2)$ problem exactly solved by a spin mean-field of the form $|\text{BCS}\rangle = e^{\sum_p t_p S_p^+} |\Downarrow\rangle$ is also exactly solved, upon JW-transformation, by a fermionic HFBF. Further, because a general HFBF is actually of the form

$$|\text{HFBF}\rangle = \left(1 + \sum_p t_p c_p^\dagger \right) e^{\sum_{p < q} \mathcal{T}_{pq} c_p^\dagger c_q^\dagger} |-\rangle, \quad (\text{S30})$$

it also proves that the mean-field solution of a JW-transformed $\mathfrak{su}(2)$ Hamiltonian is variationally bound from above by the spin mean-field solution.

ADDITIONAL PLOTS DEMONSTRATING EXTENSIVITY

We have noted in the main manuscript that our results are extensive and have shown data for the 2D J_1 - J_2 Hamiltonian to support this notion. Here we show results for the 1D XXZ model. As Fig. S1 shows, total energies/site in the fermionic mean-field behave, as a function of system size, essentially as do the results of the exact diagonalization of the spin Hamiltonian, and converge for increasing lattice sizes.

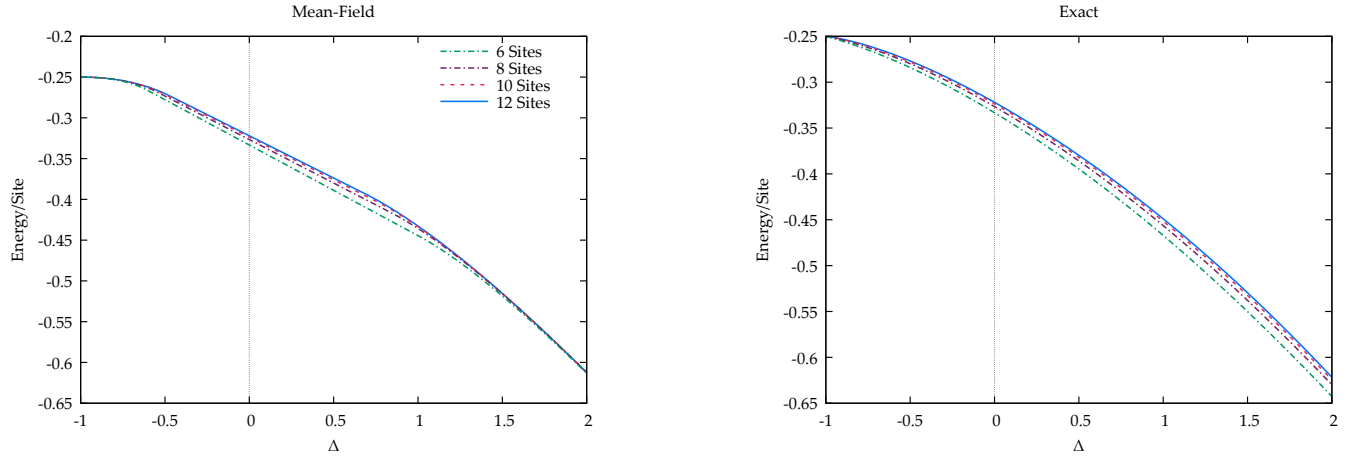


FIG. S1. Total energy per site in the 1D XXZ Hamiltonian with periodic boundary conditions, comparing the fermionic mean-field after Jordan-Wigner transformation (left panel) to the exact results (right panel).